

VYSOKÉ UČENÍ TECHNICKÉ V BRNĚ

BRNO UNIVERSITY OF TECHNOLOGY

FAKULTA ELEKTROTECHNIKY A KOMUNIKAČNÍCH TECHNOLOGIÍ

FACULTY OF ELECTRICAL ENGINEERING AND COMMUNICATION

ÚSTAV RADIOELEKTRONIKY

DEPARTMENT OF RADIO ELECTRONICS

NÁVRH A REALIZACE UHF RFID TAGU PRO SNÍMÁNÍ HLADINY KAPALINY

DESIGN AND REALIZATION OF A PASSIVE UHF RFID LIQUID LEVEL SENSOR TAG

DIPLOMOVÁ PRÁCE

MASTER'S THESIS

AUTOR PRÁCE

AUTHOR

Bc. Tomáš Pařízek

VEDOUCÍ PRÁCE

SUPERVISOR

prof. Dr. Ing. Zbyněk Raida

BRNO 2018



Diplomová práce

magisterský navazující studijní obor **Elektronika a sdělovací technika**
Ústav radioelektroniky

Student: Bc. Tomáš Pařízek

ID: 159630

Ročník: 2

Akademický rok: 2017/18

NÁZEV TÉMATU:

Návrh a realizace UHF RFID tagu pro snímání hladiny kapaliny

POKYNY PRO VYPRACOVÁNÍ:

Vypracujte přehled dostupných RFID tagů a čipů, které by bylo možné použít k měření hladiny kapaliny. Z vybraného RFID čipu a tagu snímač hladiny navrhnete a jednoduchým skriptem v MATLABu ověříte jeho účinnost. Pro snímač navrhnete novou anténu, která umožní snímat dva diskrétní stavy (dvě hladiny kapaliny) při zachování účinnosti původního systému.

Realizujte prototypy antén a propojte je s RFID čipy. Návrh senzoru ověřte simulací a experimentem (pozornost věnujte impedančnímu přizpůsobení antény k čipu). Výsledky simulace a experimentu podrobně porovnejte.

DOPORUČENÁ LITERATURA:

[1] JUN ZHANG, GUI YUN TIAN, ADI M. J. MARINDRA, ALI IMAM SUNNY, AO BO ZHAO, A review of passive RFID tag antenna-based sensors and systems for structural health monitoring applications, *Sensors*, vol. 2017, no. 2, DOI: 10.3390/s17020265

[2] A. GUILLET; A. VENA; E. PERRET; S. TEDJINI; Design of a chipless RFID sensor for water level detection, 15 International Symposium on Antenna Technology and Applied Electromagnetics, Toulouse (France): IEEE, 2012.

Termín zadání: 5.2.2018

Termín odevzdání: 17.5.2018

Vedoucí práce: prof. Dr. Ing. Zbyněk Raida

Konzultant: Jasmin Grosinger

prof. Ing. Tomáš Kratochvíl, Ph.D.
předseda oborové rady

UPOZORNĚNÍ:

Autor diplomové práce nesmí při vytváření diplomové práce porušit autorská práva třetích osob, zejména nesmí zasahovat nedovoleným způsobem do cizích autorských práv osobnostních a musí si být plně vědom následků porušení ustanovení § 11 a následujících autorského zákona č. 121/2000 Sb., včetně možných trestněprávních důsledků vyplývajících z ustanovení části druhé, hlavy VI. díl 4 Trestního zákoníku č.40/2009 Sb.

ABSTRACT

The project deals with a theoretical design of passive ultra-high frequency radio identification (UHF RFID) tag for the measurement of liquid levels. Liquid level has an influence on the input impedance of an RFID tag Antenna. The changes of input impedance have been used to distinguish individual liquid levels. Furthermore, this project presents optimization methods for the highest efficiency of an UHF RFID tag in Matlab and it aims to design a suitable Antenna within CST MICROWAVE STUDIO.

KEYWORDS

Radio Frequency Identification (RFID), UHF tag, liquid level, T-matched Antenna, optimization.

PAŘÍZEK, T. Design and realization of a passive UHF RFID liquid level sensor tag. Brno: Vysoké učení technické v Brně, Fakulta elektrotechniky a komunikačních technologií, Ústav radioelektroniky, 2018. 37s., 0 s. příloh. Diplomové práce. Vedoucí práce: prof. Dr. Ing. Zbyněk Raida

DECLARATION

Prohlašuji, že svoji diplomovou práci na téma Design and realization of a passive UHF RFID liquid level sensor tag jsem vypracoval samostatně pod vedením vedoucího diplomové práce a s použitím odborné literatury a dalších informačních zdrojů, které jsou všechny citovány v práci a uvedeny v seznamu literatury na konci práce.

Jako autor uvedené diplomové práce dále prohlašuji, že v souvislosti s vytvořením této diplomové práce jsem neporušil autorská práva třetích osob, zejména jsem nezasáhl nedovoleným způsobem do cizích autorských práv osobnostních a/nebo majetkových a jsem si plně vědom následků porušení ustanovení § 11 a následujících zákona č. 121/2000 Sb., o právu autorském, o právech souvisejících s právem autorským a o změně některých zákonů (autorský zákon), ve znění pozdějších předpisů, včetně možných trestněprávních důsledků vyplývajících z ustanovení části druhé, hlavy VI. díl 4 Trestního zákoníku č. 40/2009 Sb.

V Brně dne

.....

(podpis autora)

CONTENT

| | |
|--|-------------|
| Abstract | 1 |
| Keywords | 1 |
| DECLARATION | 3 |
| content | iv |
| list of pictures | vi |
| LIST OF TABLES | viii |
| Introduction | 1 |
| 1 RFID systems | 2 |
| 1.1 RFID Backscattering..... | 2 |
| 1.2 RFID Transponder | 3 |
| 1.2.1 Reflection coefficient..... | 4 |
| 1.2.2 Power transmission coefficient..... | 4 |
| 1.2.3 Modulation efficiency..... | 4 |
| 2 Theoretical model of Passive UHF RFID Liquid Level Sensor Tag | 6 |
| 2.1 RFID Liquid Level Sensor Tag Requirements | 6 |
| 2.2 Sensor Tag Efficiency..... | 7 |
| 2.2.1 Quality of the phase modulation α_1 | 7 |
| 2.2.2 Quality of the passive RFID chip power supply α_2 | 7 |
| 2.2.3 Quality of the backscattered tag signal α_3 | 8 |
| 2.3 Sensor Tag Optimization in Matlab..... | 8 |
| 2.3.1 Quality of the phase modulation in Matlab | 8 |
| 2.3.2 Quality of the power supply in Matlab | 10 |
| 2.3.3 Quality of the backscattered tag signal in Matlab..... | 11 |
| 2.3.4 Total efficiency of RFID sensor tag in Matlab | 11 |
| 2.4 Calculated Sensor Tag Properties..... | 12 |
| 3 Design of sensor tag Antenna | 14 |
| 3.1 Antenna Design in CST | 14 |
| 3.2 Simulation Results | 16 |

| | | |
|----------|---|-----------|
| 4 | Sensor tag antenna prototype | 19 |
| 4.1 | Antenna Measurement Method..... | 19 |
| 4.2 | Antenna from a copper tape..... | 20 |
| 4.3 | Measurement of the first prototype..... | 21 |
| 4.4 | PCB Prototype | 25 |
| 4.5 | Measurement of the second prototype | 25 |
| 5 | Water level measurement | 28 |
| 5.1 | Measurement scenario | 28 |
| 5.2 | Prototype with RFID chip UCODE 7 | 32 |
| 6 | conclusion | 35 |
| | references | 36 |
| | list of symbols and abbreviations | 37 |

LIST OF PICTURES

| | |
|--|----|
| Figure 1: Principle of backscattering [1]. | 3 |
| Figure 2: Constellation diagram of ideal RFID tag: real part of absorption coefficient versus imaginary part of absorption coefficient for case $S_{Abs}=0$ and $S_{Ref}=1$ [3]. | 5 |
| Figure 3: Ideal constellation diagram for 2 states: real part of absorption coefficient versus imaginary part of absorption coefficient. Two points of absorption mode (two sensing states) $S_{Abs}(\Delta_1)$, $S_{Abs}(\Delta_2)$ lie on circle $\tau = 0.9$ and two points of reflection mode S_{Ref} lie on circle $\tau = 0$. | 6 |
| Figure 4: Contour plot of sensing state transmission efficiency versus the Antenna impedance. | 9 |
| Figure 5: <i>Quality of the phase modulation α_1</i> versus phase difference angle. | 9 |
| Figure 6: Contour plot of the power transfer efficiency versus the Antenna impedance | 10 |
| Figure 7: <i>Quality of the power supply α_2</i> versus transmission coefficient difference.... | 10 |
| Figure 8: <i>Quality of the backscattered tag signal α_3</i> versus efficiency difference..... | 11 |
| Figure 9: <i>Total efficiency α</i> versus the Antenna impedance. | 12 |
| Figure 10: Constellation diagram after optimization in Matlab. | 13 |
| Figure 11: Scenario of level water measurement. | 14 |
| Figure 12: T-matched dipole Antenna | 15 |
| Figure 13: T-matched dipole model in CST. | 15 |
| Figure 14: Frequency response of input impedance of T-matched dipole Antenna. | 16 |
| Figure 15: Real part of Antenna impedance depends on water level. | 17 |
| Figure 16: Imaginary part of Antenna impedance depends on the water level. | 17 |
| Figure 17: Constellation diagram for final values of Antenna impedances from CST.. | 18 |
| Figure 18: Block diagram of the measurement method described in the publication (took [8]) | 19 |
| Figure 19: Comparison between simulated values, values provided by method from the publication and values achieved with help of full calibration of a balun | 20 |
| Figure 20: Prototype of the Antenna from a copper tape on the substrate Arlon 1000, Dimensions are corresponding to values from the Table 2. | 20 |
| Figure 21: Measurement probe with balun including SMA connector | 21 |
| Figure 22: Calibration setup in a controlling interface of the Mini VNA Tiny | 21 |

| | |
|--|----|
| Figure 23: VNA Calibration setup | 22 |
| Figure 24: Realization of the Open, Short and Load situations | 22 |
| Figure 25: Antenna manufactured from a copper tape on a substrate Arlon 1000. Antenna board including measure Probe. | 23 |
| Figure 26: Measurement scenario without a plastic canister. Antenna is approx 1.2 m above ground..... | 23 |
| Figure 27: Input impedance of the prototype of Antenna- Real part..... | 24 |
| Figure 28: Input impedance of the prototype of Antenna- Imaginary part..... | 24 |
| Figure 29: PCB with the Antenna Prototype which was produced by etching method . | 25 |
| Figure 30: Design of the Antenna and design of the new Measure Probe with the same feeding gap..... | 25 |
| Figure 31: Second prototype of the Antenna with the measurement probe | 26 |
| Figure 32: Input impedance of the prototype of Antenna- Real part..... | 26 |
| Figure 33: Input impedance of the prototype of Antenna- Imaginary part..... | 27 |
| Figure 34: Measurement scenario including MINI VNA TINY, Plastic Canister and Tested Antenna..... | 28 |
| Figure 35: Detail of the Antenna prototye attached on the plastic canister | 29 |
| Figure 36: Real part of impedance for two sensing states..... | 29 |
| Figure 37: Imaginary part of impedance for two sensing states | 30 |
| Figure 38: Constellation diagram for final values of Antenna impedances achiaved by measurement | 31 |
| Figure 39: Sensor tag efficiency for both sensing states..... | 31 |
| Figure 40: Final prototype with UCODE 7 chip | 32 |
| Figure 41: Simulated radiation pattern - Only Antenna , E plane (right), H plane (left) | 33 |
| Figure 42: Simulated radiation pattern - Water 5mm , E plane (right), H plane (left) . | 33 |
| Figure 43: Simulated radiation pattern - Water 30mm , E plane (right), H plane (left) . | 34 |

LIST OF TABLES

| | |
|--|----|
| Table 1: Ideal values for two sensing states obtained by Matlab | 12 |
| Table 2: Dimensions of simulated Antenna | 15 |
| Table 3: Simulated values for two sensing states obtained by CST | 17 |
| Table 4: Measured values of the input impedance for both sensing states | 30 |

INTRODUCTION

The aim of the project was to identify state-of-the-art ultra-high frequency (UHF) RFID chips which are suitable for measurement of two water levels [1]. The RFID tags have been selected with respect to individual parameters, such as no integrated adaptive matching, available data of input impedance versus frequency and power, amplitude modulation of backscatter signal and, last but not least, handy package dimensions for easy soldering.

The following part of the project describes the optimization of sensor tag efficiency and analyses a suitable selection of two sensing conditions. For a well-functioning RFID tag it is important to define and maximize sensor sensitivity, wireless power transfer and modulation efficiency. That optimization has been done in Matlab.

Furthermore, the project shows the design of a T-matched dipole Antenna to sense two discrete sensing states (two water filling levels) with regard to high performance in terms of sensor tag efficiency. Optimization of the Antenna has been done in CST Microwave Studio.

1 RFID SYSTEMS

Radio Frequency Identification (RFID) is a system of everyday use. Currently, RFID tags are used in many sectors like industries, shopping, pharmacy, and identification of animals. The first mention of RFID is dated as late as 1945 [2], but the first patent was granted to an American scientist Charles Walton in 1983. Nowadays the RFID systems have many forms using different frequency bands. RFID systems can operate in low frequency (LF) bands, high frequency (HF) bands and UHF bands. Relatively newly, RFID tags operate in microwaves bands.

LF RFID systems operate at the frequency 125 kHz. These 125 kHz low frequency RFID tags are used for identifying employees at entrance ways and secured rooms of offices, for instance. Small in size, tags are easy to carry and use.

HF RFID Tags operate at frequency 13.56 MHz. This HF thin card tag features fast response speeds and is intended for ticketing and payment applications, access control and asset tracking.

UHF RFID Tags operate at frequency 865 to 868 MHz (US 902 to 928 MHz). These are a variety of tags including those designed for temperature and humidity sensing or on metal mounting and built to be rugged and tamper-proof.

RFID systems which use microwaves band operate at frequency 2.45 GHz. Some common applications of 2.45 GHz RFID tags are auto dealerships, personnel tracking, asset tracking, access control etc.

The basic differences between described technologies comprise range of the tags and principle of communication (magnetic field versus electromagnetic waves). More details are available in [6].

RFID systems consist of two basic parts: a reader and a tag. Readers are used for detection and communication between tags. We can say that an RFID reader is a sensor which senses information from RFID tags. The reader also allows to write/send some information to the RFID tag. An RFID tag is attached to the objects to identify them. The RFID tag stores information about objects in memory and this information can be transmitted to the reader. RFID tags are divided into three basic classes depending on the type of power supply:

- Actives tags need external power supply, for instance, from some kind of a battery.
- Passive tags take power from RFID reader.
- Semi-passive tags need battery for power electronics but not for communication between the tag and the reader.

1.1 RFID Backscattering

The effect of backscattering is used with passive and semi-passive tags. The principle of this phenomenon is hidden in the fact that the tag reflects the RF signal transmitted by the reader. An Antenna is connected to a chip and the chip operates as a switch between two

states. Hence, the Antenna is attached to the ground (reflection model) or to an absorption impedance chip (absorption model). The result of this behaviour is a modulated tag response representing some information (e.g. ID, etc.)

Basic sketch of RFID system using backscattering is depicted in Figure 1.

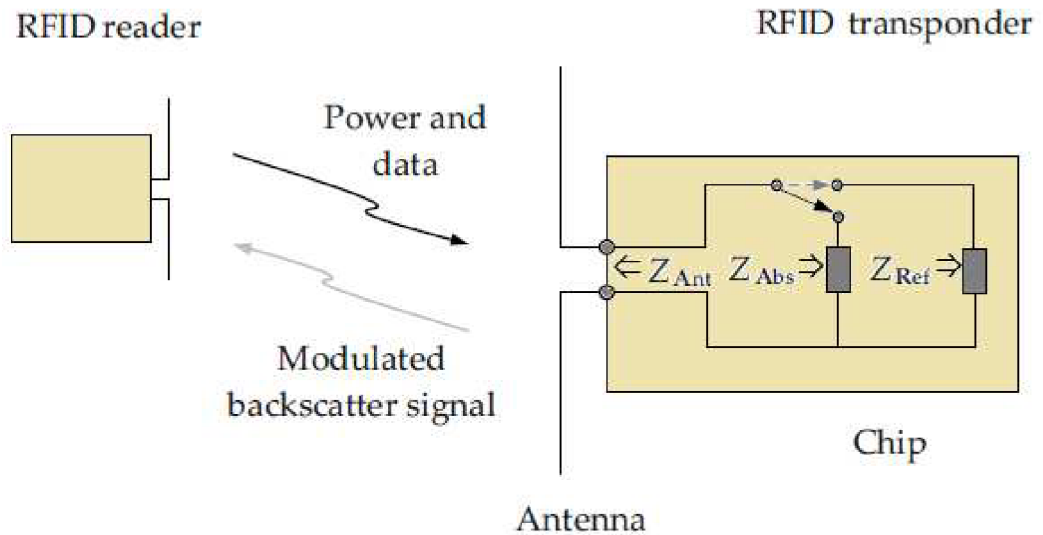


Figure 1: Principle of backscattering [1].

In Figure 1, three different impedances Z_{Ref} , Z_{Abs} and Z_{Ant} are shown:

- Z_{Ref} is the reflection impedance of the RFID chip. In an ideal case this impedance is 0Ω , but the real value of reflection impedance is about $(2+0.1j) \Omega$.
- Z_{Abs} is the absorption impedance. This is usually the same impedance like the RFID chip input impedance. The absorption impedance can depend on the package of the RFID chip, and the type of the RFID chip which value is not 50Ω like by many RF components. The absorption impedance has usually a high negative imaginary part, for instance $(20-250j) \Omega$.
- Z_{Ant} represents the impedance of the Antenna. The Antenna impedance together with the absorption impedance influences the reflection coefficient. For maximum power transfer, the Antenna impedance has to be a complex conjugate value of the absorption impedance. Relationships between impedances are described below.

1.2 RFID Transponder

The RFID transponder is a combination of an RFID chip and an Antenna. The behaviour of a transponder is described by three parameters:

- Reflection coefficient,
- Power transmission coefficient,
- Modulation efficiency.

1.2.1 Reflection coefficient

The reflection coefficient describes the ability of an RFID transponder to absorb or reflect energy. The reflection coefficient is defined as: [1]

$$S = \frac{Z_L - Z_S^*}{Z_L + Z_S} \quad [-] \quad (1)$$

Here, Z_L is the load impedance, Z_S the source impedance and Z_S^* is the complex conjugate source impedance.

In view of the RFID transponder, we can write a relationship for two different reflection coefficients – for the absorption mode S_{Abs} and the reflection mode S_{Ref} [1]:

$$S_{Abs} = \frac{Z_{Abs} - Z_{Ant}^*}{Z_{Abs} + Z_{Ant}} ; S_{Ref} = \frac{Z_{Ref} - Z_{Ant}^*}{Z_{Ref} + Z_{Ant}} \quad [-] \quad (2)$$

In an ideal case, we want to achieve $S_{Abs}=1$ (the transponder is ideally matched to the Antenna) and $S_{Ref}=0$ (the Antenna is totally un-matched and a maximum reflection occurs).

1.2.2 Power transmission coefficient

The behavior of the RFID transponder can be described by the power transmission coefficient [1]:

$$\tau = 1 - |S_{Abs}|^2 = \frac{4R_{Abs}R_{Ant}}{|Z_{Abs} + Z_{Ant}|^2} \quad [-] \quad (3)$$

Here, S_{Abs} is the absorption coefficient described above, R_{Abs} is the real part of the absorption impedance, and R_{Ant} is the real part of Antenna impedance. Z_{Abs} and Z_{Ant} denote the absorption impedance and the Antenna impedance.

The power transmission coefficient τ ranges from 0 to 1:

- If $\tau=1$, the RFID transponder is fully matched.
- If $\tau=0$, the RFID transponder is fully unmatched and no power is transmitted.

1.2.3 Modulation efficiency

The modulation efficiency η is a measure of the modulation quality of the tag signal. The efficiency is defined as a vector distance between two states (S_{Abs} and S_{Ref}) [1]:

$$\eta = \frac{2}{\pi^2} |S_{Abs} - S_{Ref}|^2 \quad [-] \quad (4)$$

Here, S_{Abs} is the absorption coefficient and S_{Ref} is the reflection coefficient. The maximum

value of the modulation efficiency is about 0.2 for the tag, which uses amplitude modulation.

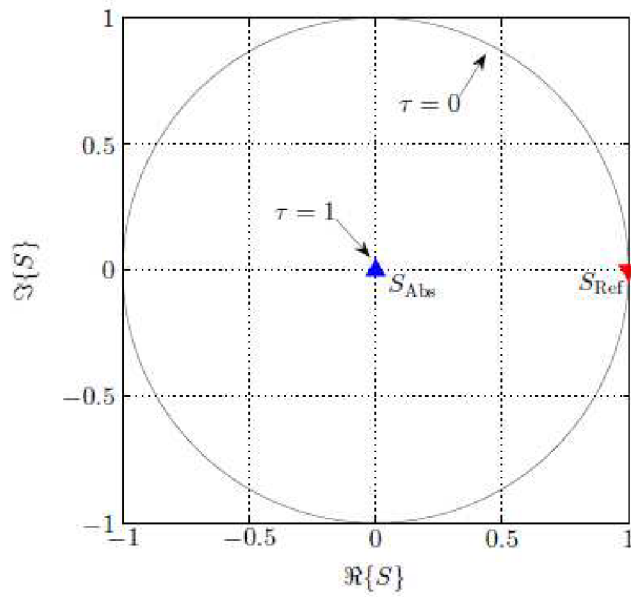


Figure 2: Constellation diagram of ideal RFID tag: real part of absorption coefficient versus imaginary part of absorption coefficient for case $S_{Abs}=0$ and $S_{Ref}=1$ [3].

Figure 2. shows a constellation diagram where the real part of the absorption coefficient lies on the x axis and the imaginary part of the absorption coefficient lies on the y axis. In the centre of the constellation diagram, the point S_{Abs} corresponds with the ideally matched RFID transponder. On the right-hand side, the reflection-mode point is located. If we substitute values from the constellation diagram to equation 2, we get the modulation efficiency of just around 0.2 for the amplitude-modulated tag.

2 THEORETICAL MODEL OF PASSIVE UHF RFID LIQUID LEVEL SENSOR TAG

This chapter describes a suitable selection of sensing states for achieving higher efficiency of the sensor tag [3]. Further, it presents a selection of suitable Antenna impedances for individual liquid levels. These optimizations have been done in Matlab.

2.1 RFID Liquid Level Sensor Tag Requirements

The liquid sensor should be able to distinguish two different levels of water. Thus, that sensor has two different sensing states Δ_1 and Δ_2 . This is very important for the total resolution (between each sensing state, very high phase shift can be expected).

Sufficiently high and constant transmission coefficient τ is the next requirement which guarantees the chip operation for all sensing states.

Sufficiently high and stable modulation efficiency for all sensing states is other requirement which allows distinguishing two water states from different values of the sensor Antenna impedance.

The frequency band of operation was selected being 915 MHz. And of course, the sensor tag efficiency is needed as high as possible.

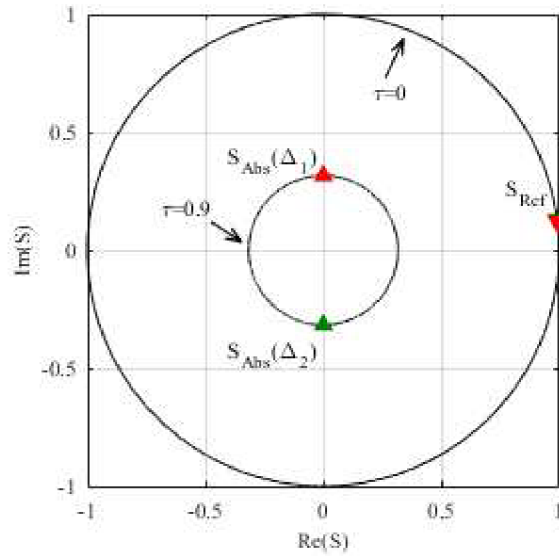


Figure 3: Ideal constellation diagram for 2 states: real part of absorption coefficient versus imaginary part of absorption coefficient. Two points of absorption mode (two sensing states) $S_{Abs}(\Delta_1)$, $S_{Abs}(\Delta_2)$ lie on circle $\tau = 0.9$ and two points of reflection mode S_{Ref} lie on circle $\tau = 0$.

Figure 3 shows an ideal constellation diagram with two sensing states. The phase difference between sensing states is a 180° that is very important for the total efficiency of the RFID tag (described below). For the total efficiency, it is also important to have the same distance $S_{Abs}(\Delta_k)$ and $S_{Ref}(\Delta_k)$.

2.2 Sensor Tag Efficiency

The sensor tag efficiency α describes the total efficiency depending on the quality of the phase modulation, quality of the passive RFID chip power supply and quality of the backscattered tag signal. The sensor tag efficiency is defined as [6]:

$$\alpha = \sqrt[3]{\alpha_1 \alpha_2 \alpha_3} \quad [-] \quad (5)$$

Here, α_1 is the quality of the phase modulation, α_2 is the quality of the passive RFID chip power supply and α_3 the quality of the backscattered tag signal. The sensor tag efficiency lies within $\langle 0, 1 \rangle$. In an ideal case, $\alpha=1$.

2.2.1 Quality of the phase modulation α_1

This parameter describes the phase difference in degrees between each sensing state $S_{Abs}(\Delta_k)$. The parameter α_1 has an influence on the distinguishability of different sensing states. According to [3], the maximum value of sensing states for reliable distinguish is 4. The formula is defined as [1]:

$$\alpha_1 = \frac{\Delta\phi_{Min}}{360^\circ/K} \quad (6)$$

Here $\Delta\phi_{min}$ is the minimum phase difference in degrees and K is the number of sensing states. In ideal case, $\alpha_1=1$.

2.2.2 Quality of the passive RFID chip power supply α_2

This parameter provides information about the power supply of the passive RFID chip defining Antenna impedances which lie on the circle corresponding with transmission coefficient $\tau=0.9$ (in Figure 3) [1a]. The parameter α_2 is defined as [1]:

$$\alpha_2 = 1 - \beta |\tau_{Ref} - \tau(\Delta_k)|_{Max} \quad [-] \quad (7)$$

Here, β is a weighting factor lying within $(0, 10 \rangle$, τ_{ref} is the reference value of the transmission coefficient and $\tau(\Delta_k)$ is the transmission coefficient for each sensing state.

A weighting factor is a weight given to a data point to assign it a lighter, or heavier, importance in a group. The factor is usually used for calculating a weighted mean, to give less (or more) importance to group members. In that case, the weighting factor β is used to balance the influence of the power transfer efficiency α_2 on α . If the factor increases the value of β , the value of α_2 is decreased. Thus, the influence of α_2 on the sensor tag efficiency decreases (and vice versa).

Reference value of the transmission coefficient τ_{ref} describes the circle in the constellation diagram on which the absorption coefficients lie for each sensing state.

2.2.3 Quality of the backscattered tag signal α_3

This parameter says that each sensing state should have the same distance vector between $S_{Abs}(\Delta_k)$ and S_{Ref} . Thus, the efficiency of individual sensing states should be the same. In this case, $\alpha_3=1$. Quality of the backscattered tag signal is defined as [7]:

$$\alpha_3 = 1 - \beta_2 |\eta_k - \eta_{i \neq k}|_{Max} \quad (8)$$

Here, β_2 is the weighting factor, and η_k is efficiency of the state $S_{Abs}(\Delta_k)$. The weighting factor β_2 is used to balance the influence of the power transfer efficiency α_3 on α .

2.3 Sensor Tag Optimization in Matlab

As a reference chip, the RFID chip SL3S1204 UCODE 7 [4] was selected:

- The absorbing impedance of the chip in the SOT package at the frequency 915 MHz is $Z_{Abs} = (12.8 - 248j) \Omega$.
- The reflection impedance was selected as $Z_{Ref} = (2 - 0.1j) \Omega$.

These parameters have been used as input parameters of the Matlab optimization script. Other input parameters follow:

- Weighting factors β_1 and β_2 (both = 1),
- The number of sensing states K ,
- The reference value of power transmission coefficient $\tau_{ref} = 0.9$.

Outputs of the optimization MATLAB script are:

- Suitable Antenna impedances for two states,
- Plots showing dependency of efficiencies (α_1 , α_2 and α_3) on input Antenna impedance.

2.3.1 Quality of the phase modulation in Matlab

Figure 4 shows dependency of quality of the phase modulation α_1 on the Antenna impedance. The plot shows all possible Antenna impedances for states $S_{Abs}(\Delta_1)$ and $S_{Abs}(\Delta_2)$ between which the phase difference is 180° . This means that values of impedances, which are located in red area, are associated with the phase difference of states, which is very close to 180° .

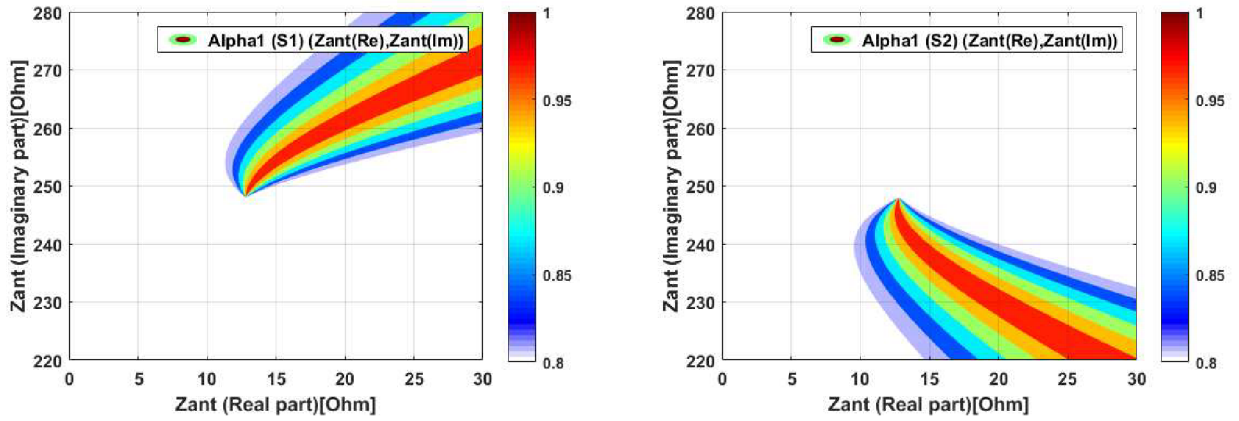


Figure 4: Contour plot of sensing state transmission efficiency versus the Antenna impedance.

For instance, the value $(20 + 260j) \Omega$ from the first plot (Figure 4 left) has the phase shift $\sim 180^\circ$ with the value $(20 + 230j) \Omega$ from the second plot (Figure 4 right).

Figure 5 shows the dependency of the quality of the phase modulation α_1 on the phase difference. Obviously, the increase of the phase difference (interval from 0° to $\pm 180^\circ$) increases α_1 up to 1. In the ideal case, the value of $\alpha_1 = 1$. Thus, the phase difference is 180° , and is possible distinguish between two states without any major problems. If the value of phase difference is very small, we are not able to distinguish between two sensing states. In the worst case $\alpha_1 = 0$, the phase difference between two sensing states is 0° .

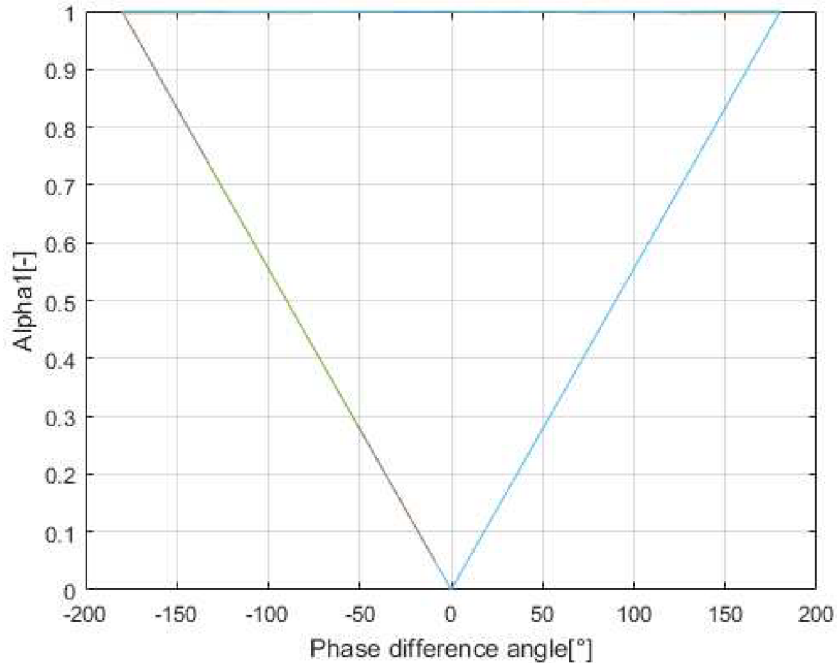


Figure 5: Quality of the phase modulation α_1 versus phase difference angle.

2.3.2 Quality of the power supply in Matlab

Figure 6 shows the dependency of the quality of the passive RFID chip power supply α_2 on Antenna impedance. The plot shows a circular area (the red circle) which corresponds to the reference level of the power transmission coefficient $\tau_{\text{ref}} = 0.9$.

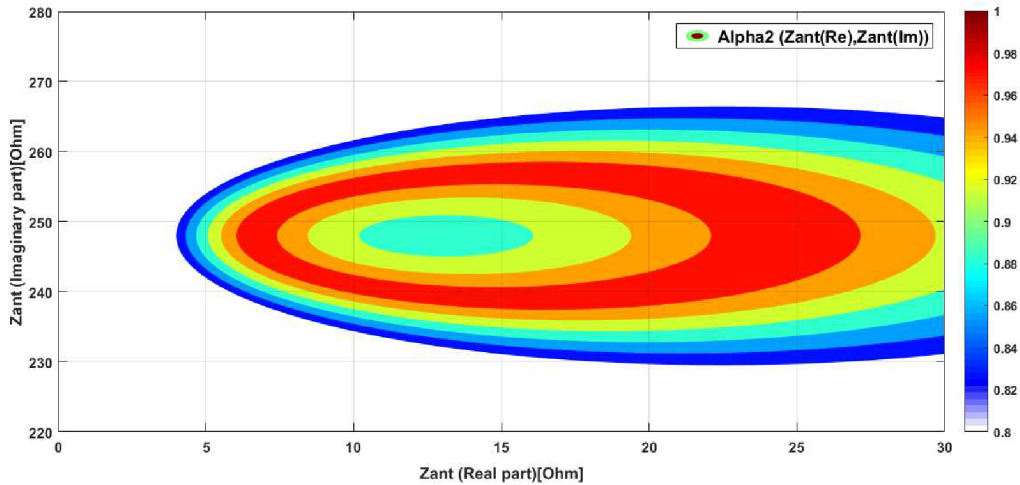


Figure 6: Contour plot of the power transfer efficiency versus the Antenna impedance

Figure 7 represents the dependency of the quality of the passive RFID chip power supply α_2 on the transmission coefficient difference. The transmission coefficient difference is a difference between τ_{ref} and $\tau(\Delta_k)$. If the difference is increased, the value of α_2 is decreasing. The ideal case occurs if the difference is 0. Thus, $\alpha_2 = 1$.

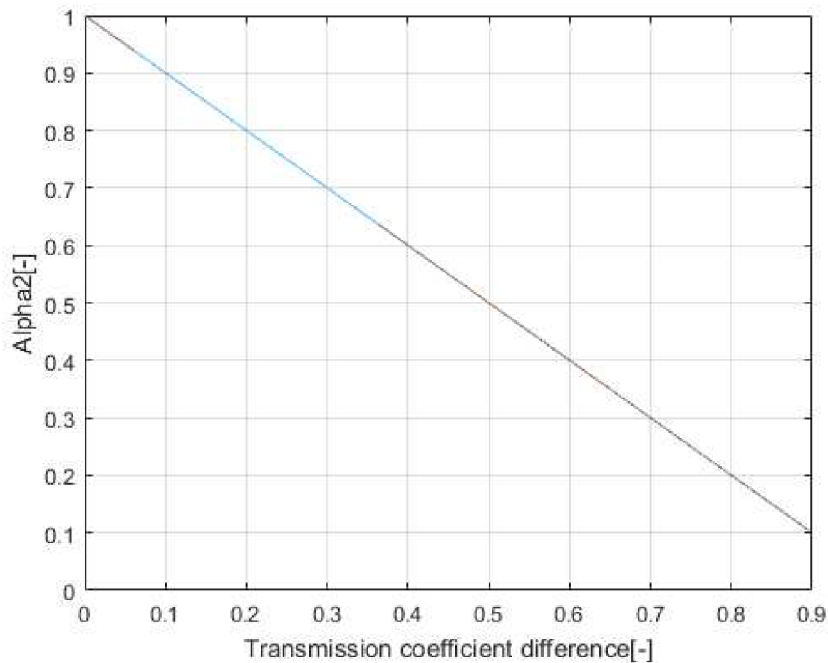


Figure 7: Quality of the power supply α_2 versus transmission coefficient difference.

2.3.3 Quality of the backscattered tag signal in Matlab

Plot 8 represents dependency quality of the backscattered tag signal α_3 versus efficiency difference. Increasing level of difference causes decreasing of α_3 . In an ideal case it is necessary ensure that efficiency difference is 0.

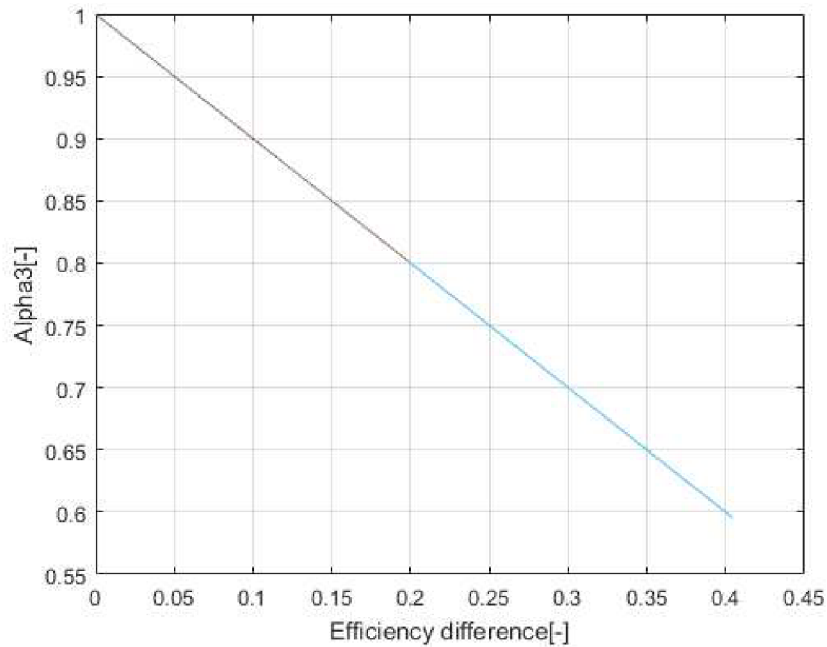


Figure 8: Quality of the backscattered tag signal α_3 versus efficiency difference.

2.3.4 Total efficiency of RFID sensor tag in Matlab

Previous chapters described the way of calculating individual components of the total efficiency α . In the last step, all parameters described above have been connected into a single contour plot using a MATLAB script. That contour plot shows the dependency of the total efficiency of the RFID sensor tag on input impedance of the Antenna. The red areas in the plot show the most appropriate input impedances of the Antenna. This plot is used to select suitable Antenna impedances for simulation in CST Microwave Studio.

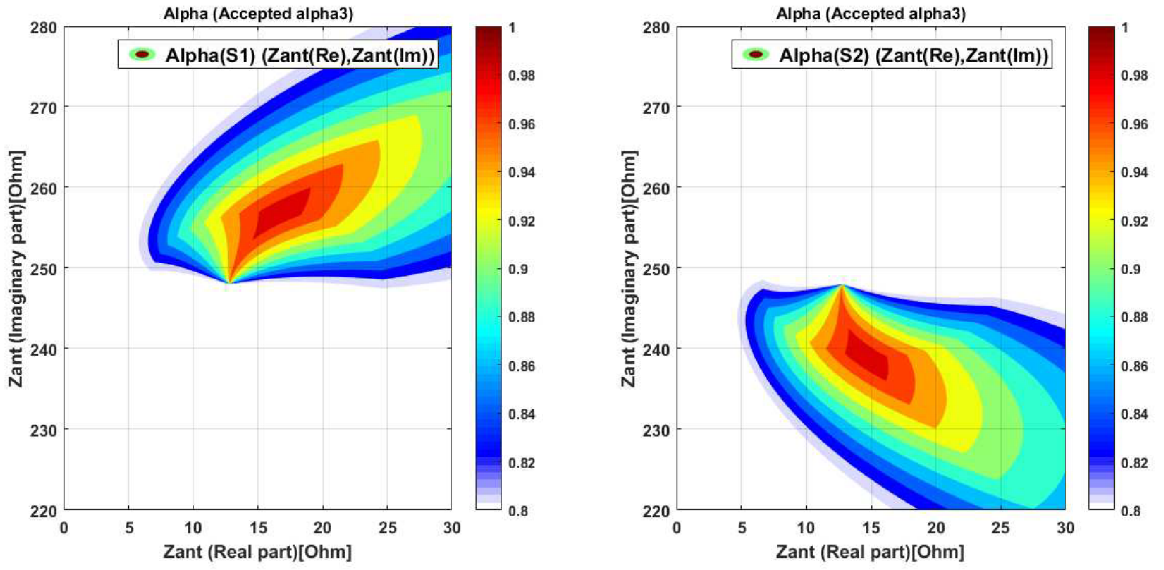


Figure 9: Total efficiency α versus the Antenna impedance.

2.4 Calculated Sensor Tag Properties

The optimization has been done in Matlab. Antenna impedances, the power transmission coefficient, phase of the absorbing reflection and the modulation efficiency for each sensing state are the outputs of the Matlab script (see Table 1).

Table 1: Ideal values for two sensing states obtained by Matlab

| Sensing state | Z_{ant} [Ω] | τ [-] | ϕ_{abs} [$^\circ$] | η [-] |
|---------------|------------------------|------------|---------------------------|------------|
| Δ_1 | $16.7 + 256.9j$ | 0.9 | 90 | 0.22 |
| Δ_2 | $14.55 + 239.1j$ | 0.9 | 270 | 0.22 |

Table 1 shows parameters of the sensor tag which have been computed in Matlab. Impedance for each sensing state is related to another one with the phase difference 180° . Both Antenna impedances lie on the circle for $\tau=0.9$. The ideal efficiency for both sensing states is 22%. Figure 10 shows a constellation diagram for the ideal case.

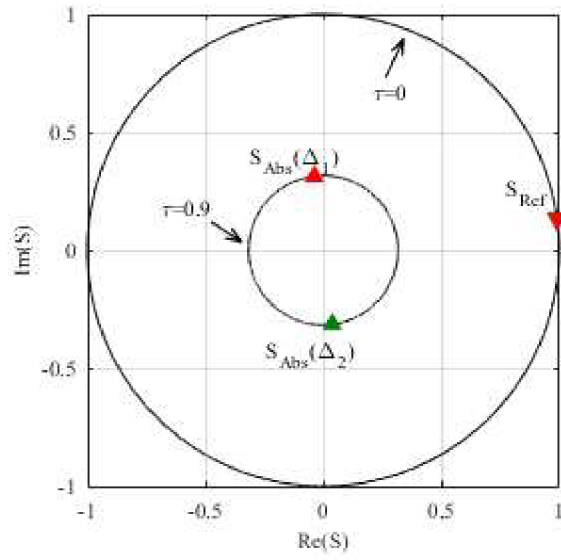


Figure 10: Constellation diagram after optimization in Matlab.

3 DESIGN OF SENSOR TAG ANTENNA

In this chapter, the design of the Antenna for the sensor tag is described. As a suitable Antenna, the T-matched dipole [5] was chosen: the T-matched dipole provides a high freedom in the impedance matching for specific RFID chip impedance. The T-matched dipole has been designed in CST MICROWAVE STUDIO.

3.1 Antenna Design in CST

Requirements on the Antenna parameters are given in Table 1. The Antenna designed in CST Microwave Studio consists of the T-matched dipole, which was etched from the copper foil (thickness 35 μm) on the ARLON1000 substrate (thickness 0.8 mm, dielectric constant $\epsilon_r = 10.2$). The substrate with the Antenna layout is attached to a plastic water container made of the PE-HD material. In the water container, there is a variable level of water which influences the input impedance of the dipole. The described scenario is sketched in Figure 11.

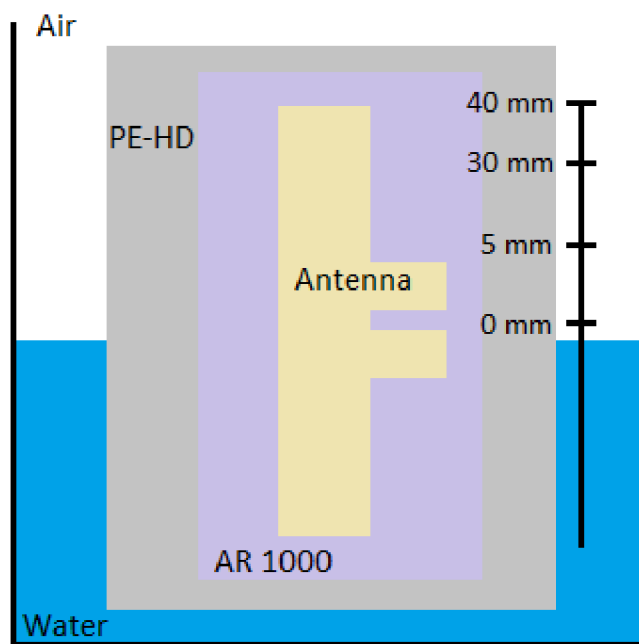


Figure 11: Scenario of level water measurement.

The water has a relative permittivity $\epsilon_r = 78$ and the PE-HD is of the permittivity $\epsilon_r = 2.3$. Thickness of the plastic water container is 1 mm. Thickness of water for simulation was chosen 5 mm. Simulations in CST showed that a larger thickness has no influence on the input impedance of the Antenna.

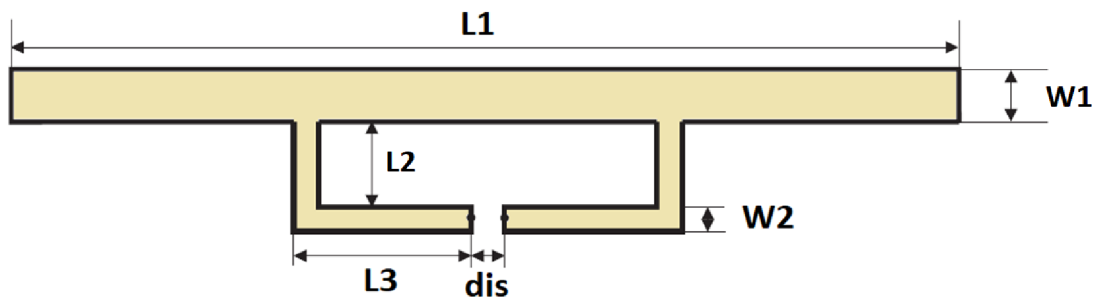


Figure 12: T-matched dipole Antenna

Table 2: Dimensions of simulated Antenna

| L1 [mm] | L2 [mm] | L3 [mm] | W1 [mm] | W2 [mm] | dis [mm] |
|---------|---------|---------|---------|---------|----------|
| 80.00 | 20.03 | 8.50 | 12.00 | 1.04 | 0.4 |

Figure 13 shows the designed T-matched dipole in CST. The resonant frequency of the Antenna was tuned for the full level of water in the plastic container (the level of water 40 mm). Changing parameters L2, W2 and dis, real and imaginary parts of input impedance of the Antenna was changed. Dimensions of the substrate are $W = 48$ mm and $L = 90$ mm.

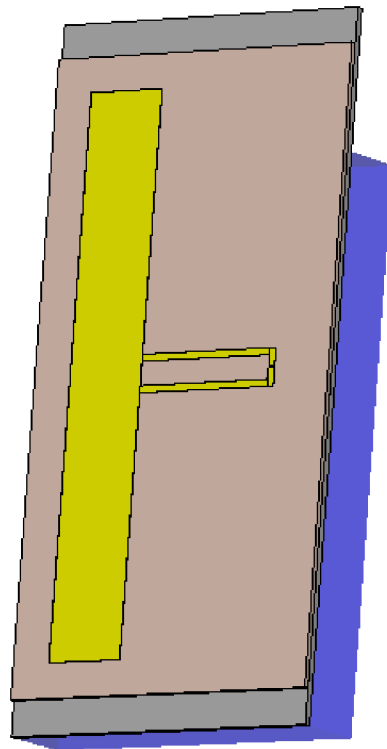


Figure 13: T-matched dipole model in CST.

The Antenna was simulated in CST Microwave Studio. The search for two different impedances is very tricky, because the dependency of the Antenna impedances on the water level is nonlinear. Therefore, searching for just two ideal values is difficult using the Matlab script described above. So the search was aimed to find values near to Matlab ones, keeping the condition of the highest sensor tag efficiency.

3.2 Simulation Results

Figure 14 shows the real and imaginary part of the Antenna impedance in frequency range 500 MHz to 3 GHz. The resonant frequency of the Antenna (1800 MHz) was tuned for the full level of water in a plastic container (the water level 40 mm).

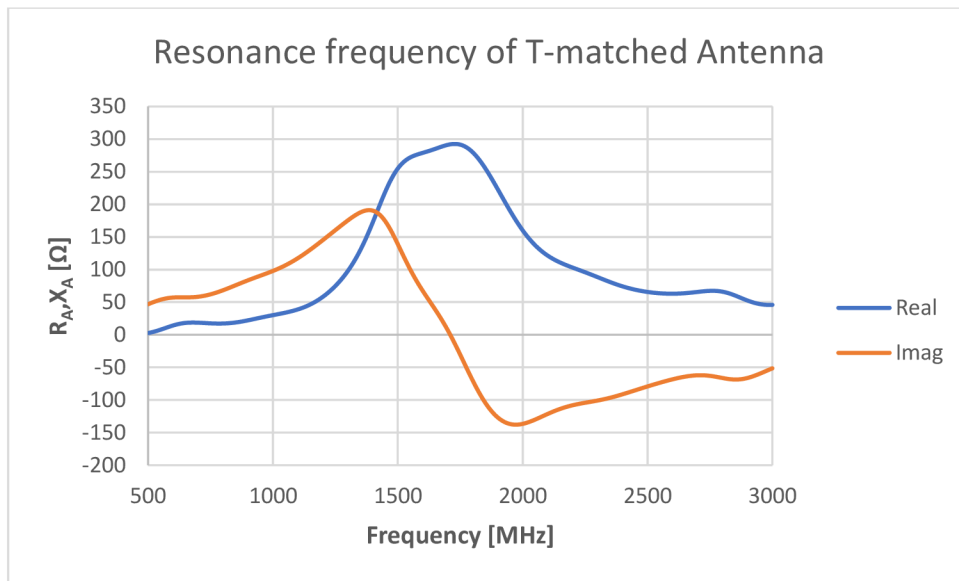


Figure 14: Frequency response of input impedance of T-matched dipole Antenna.

Water levels of 5 mm and 30 mm were selected as the measured states. For these levels, CST simulations were done. Results of these simulations are shown in Figures 15, 16.

Figure 15 shows the real part of the Antenna impedance when the water level was changed from 5 mm to 30 mm. In both water levels at the frequency of 915 MHz, the real part of input impedance the Antenna has the same value 16.7 Ω.

Figure 16 shows the imaginary part of the Antenna impedance when the water level was changed from 5 mm to 30 mm. At the frequency 915 MHz, the imaginary part of Antenna impedance is different for both water levels. For the water level 5 mm, the reactance is 256j Ω, and for 30 mm, the reactance equals to 242.5j Ω.

In Figures 15 and 16, changes of input impedance depending on the water level are observable. Obtained input impedances for both sensing states are described in Table 3. For those impedances, transmission coefficient τ , phase difference ϕ_{abs} and total efficiency η have been done calculated.

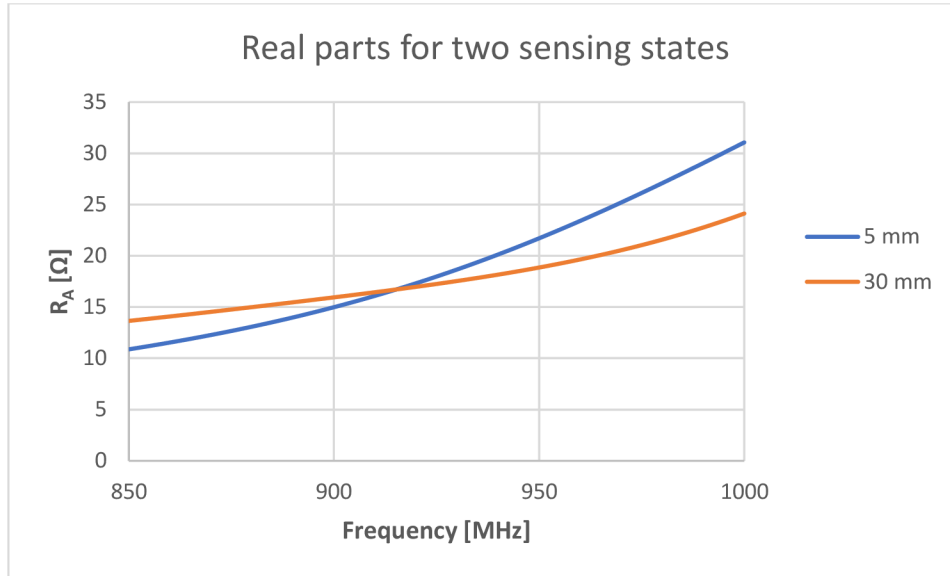


Figure 15: Real part of Antenna impedance depends on water level.

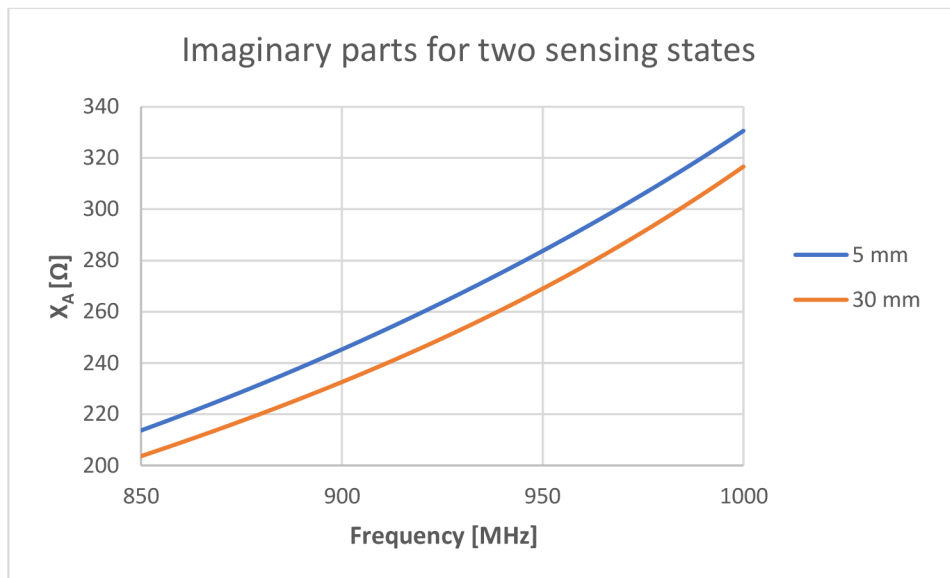


Figure 16: Imaginary part of Antenna impedance depends on the water level.

Table 3: Simulated values for two sensing states obtained by CST

| Sensing state | Z_{ant} [Ω] | τ [-] | ϕ_{abs} [$^\circ$] | η [-] |
|---------------|------------------------|------------|---------------------------|------------|
| Δ_1 | 16.7+256j | 0.915 | 90 | 0.226 |
| Δ_2 | 16.7+242j | 0.943 | 237 | 0.261 |

The designed Antenna shows very good sensor tag efficiency, with τ values close to the reference values, a phase difference of 147° . Efficiency for each sensing state is more than 20%. However, the value of the phase difference should distinguish reliably between the two sensing states. Results from Table 3 are show in constellation diagram in Figure 17.

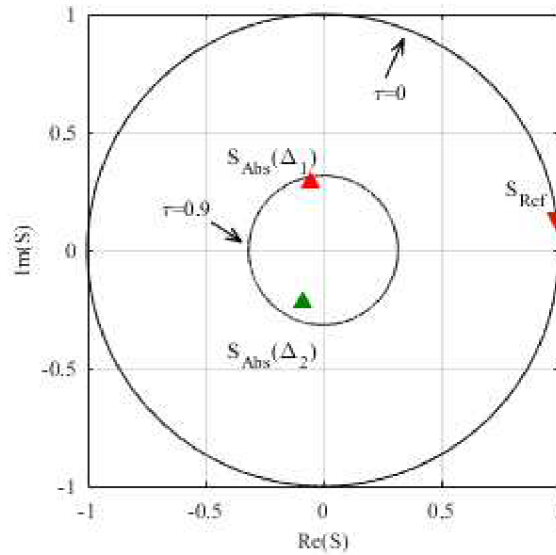


Figure 17: Constellation diagram for final values of Antenna impedances from CST.

Figure 17 shows the constellation diagram with two sensing states. These sensing states correspond to two impedance values which have been obtained by optimization in CST Microwave Studio.

4 SENSOR TAG ANATENNA PROTOTYPE

This chapter describes manufacturing of Antenna prototypes for the RFID sensor. The first prototype has been done with the help of a copper tape. The second prototype has been manufactured by an etching method.

4.1 Antenna Measurement Method

For measurement of the Antenna prototypes, it was necessary to define a measurement method. I decided to use a method which uses one port of a VNA. These methods most often use a balun. One method, which uses balun for impedance measurement of balanced Antennas is describes in [8].

Principle of this method is shown in the picture 18. By a VNA are connected different impedances and with help of equation which is described in the publication [8] is computed total value of input impedance of an Antenna.

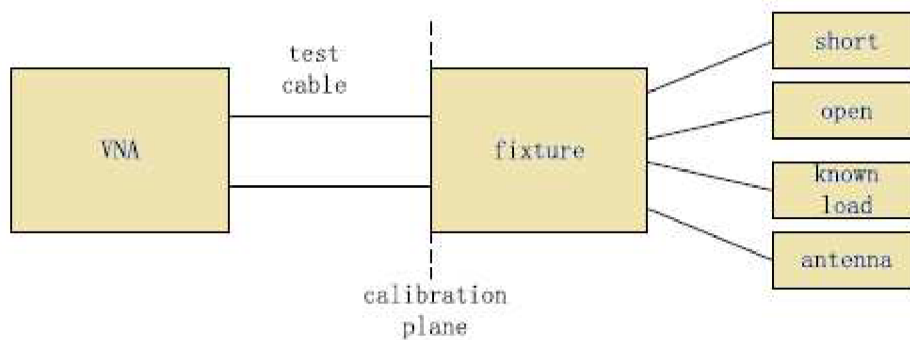


Figure 18: Block diagram of the measurement method described in the publication (took [8])

This method has been compared with full balun calibration. It means, that calibration plane was shifted behind a fixture (balun). These two methods has been compared and results were shown to the plots. As reference Antenna for measurement has been used Antenna described below.

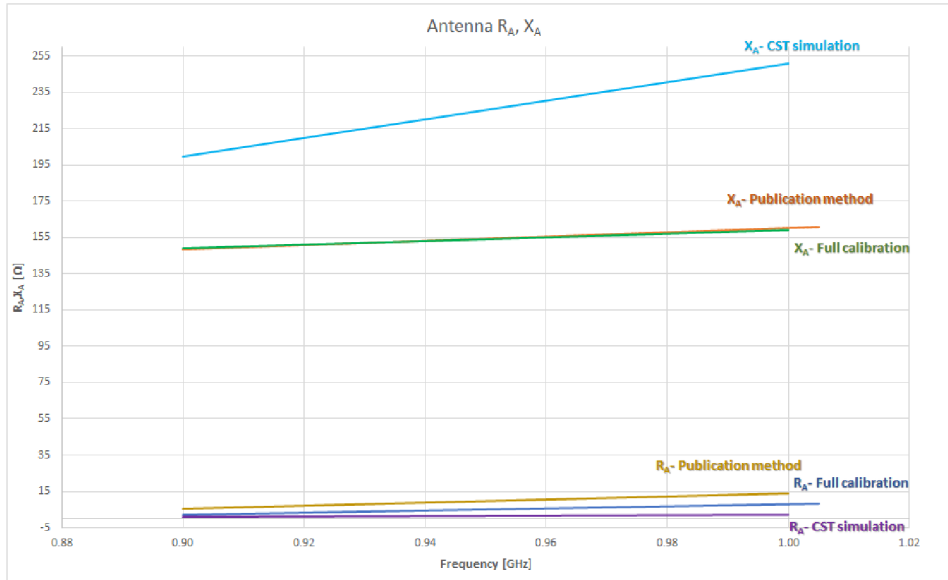


Figure 19: Comparison between simulated values, values provided by method from the publication and values achieved with help of full calibration of a balun

In the Figure 19 are shown results of the input impedance which were achieved with help of different calibration setup. Achieved results for full calibration method and method described in the publication are very close Because is measurement with full calibration more flexible and faster, so was used just this method.

4.2 Antenna from a copper tape

For this prototype a copper tape with thickness 35 μm and substrate Arlon 1000 has been used. For achievement of accurate shape a scalpel has been used. Dimensions of the Antenna are corresponding to values which were achieved from CST Microwaves Studio (Table 2).

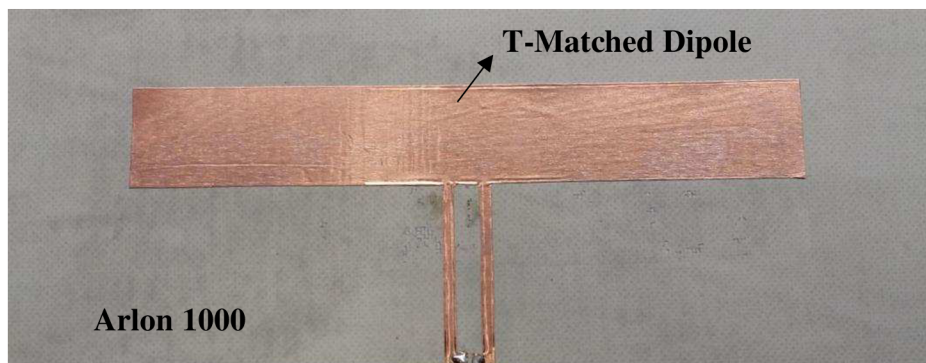


Figure 20: Prototype of the Antenna from a copper tape on the substrate Arlon 1000, Dimensions are corresponding to values from the Table 2.

4.3 Measurement of the first prototype

The Antenna has a symmetrical feeding, so it was necessary to choose some suitable method for a measurement. As measurement method has been chosen a method which uses a balun (describes above). The balun works like convertor between symmetrical and asymmetrical transmission lines. For measurement a balun provided by Johanson Technology [9] with frequency range from 800 MHz to 1000 MHz has been used. This BALUN is in the SMD 1206 package.

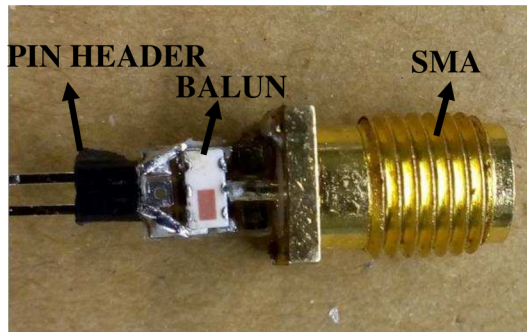


Figure 21: Measurement probe with balun including SMA connector

Measurement has been done with help of miniVNA Tiny [9], that is one port USB VNA with range up to 3 GHz. Before measurement was the balun calibrated to the reference value of 50 Ω . For accurate calibration 10000 calibration steps has been chosen (Figure 22).

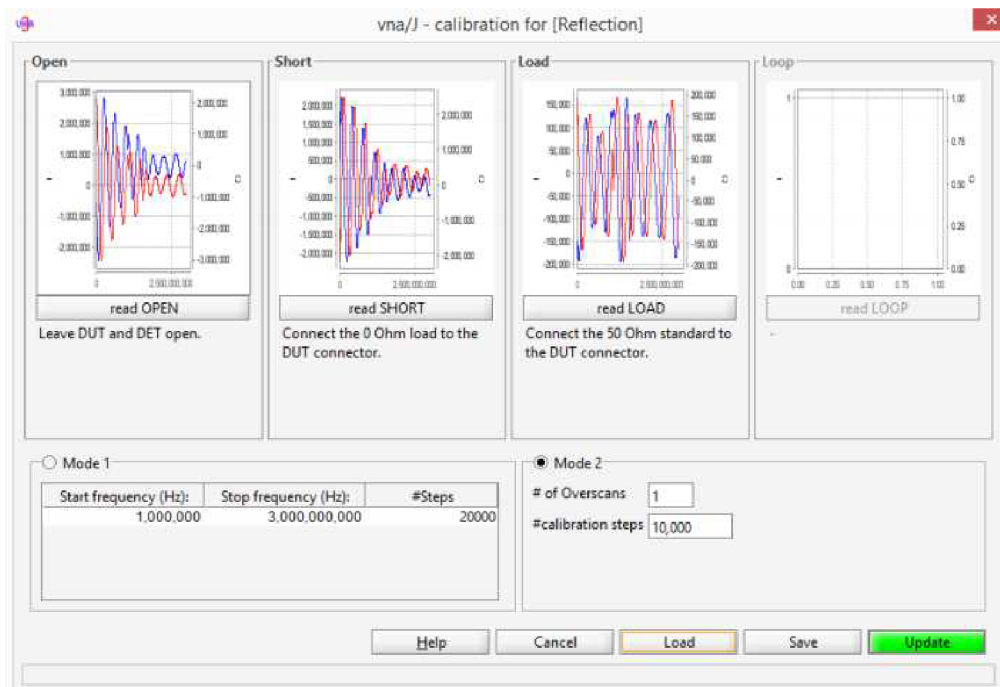


Figure 22: Calibration setup in a controlling interface of the Mini VNA Tiny

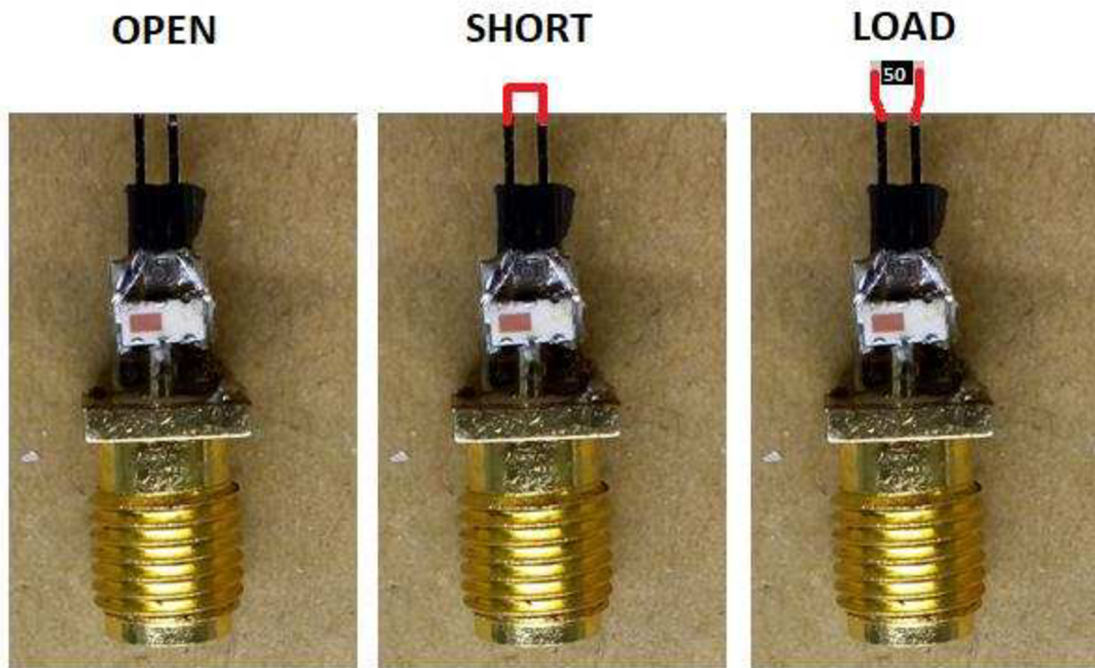


Figure 23: VNA Calibration setup

In the picture 23 is shown theoretical calibration setup. Short was realized with help of a soldering station, load situation was realized with 50 Ohm SMD resistor, which was soldered to the pin header. Illustration situation is shown in the picture 24.



Figure 24: Realization of the Open, Short and Load situations

After calibration was the measurement probe to solder to the Antenna. And with help of VNA the measurement of input impedance of Antenna has been done.

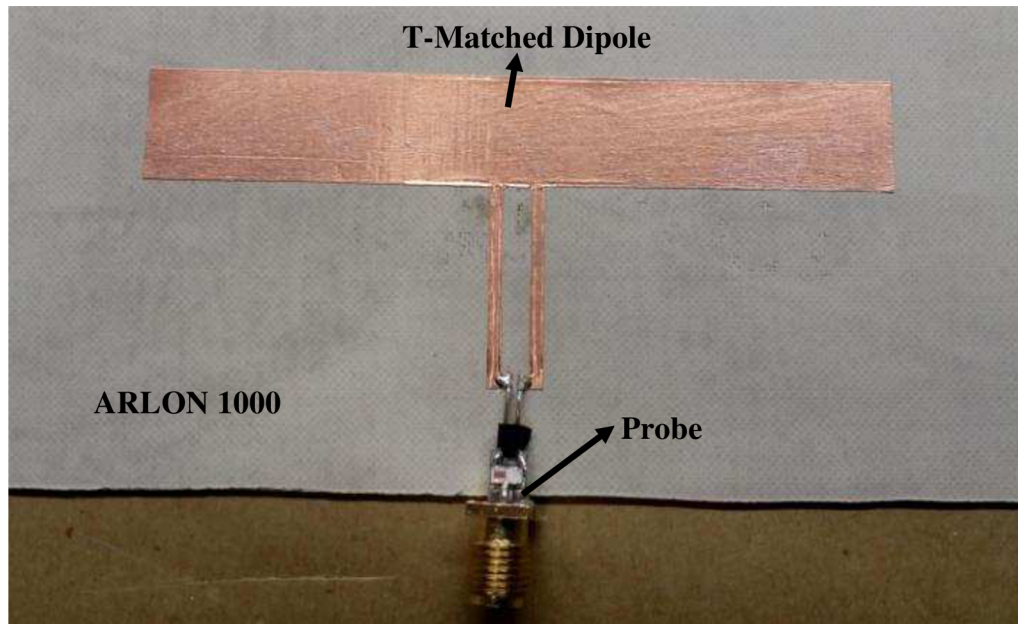


Figure 25: Antenna manufactured from a copper tape on a substrate Arlon 1000. Antenna board including measure Probe.

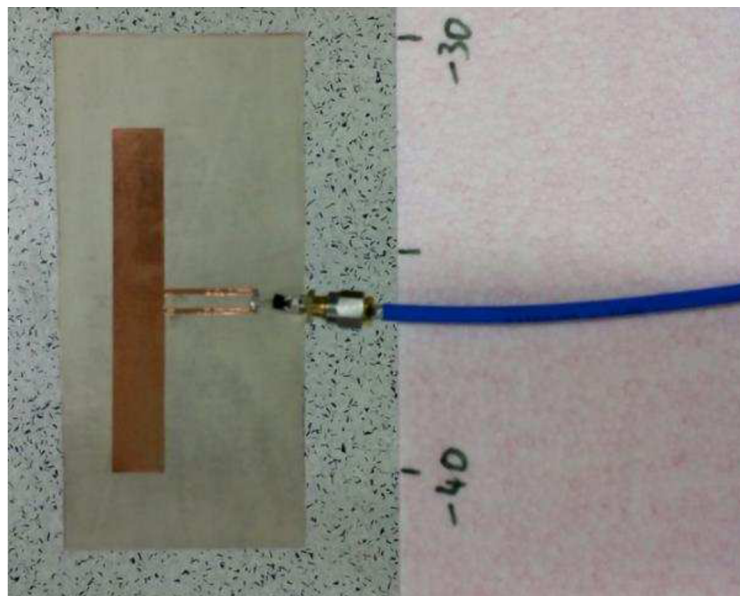


Figure 26: Measurement scenario without a plastic canister. Antenna is approx 1.2 m above ground.

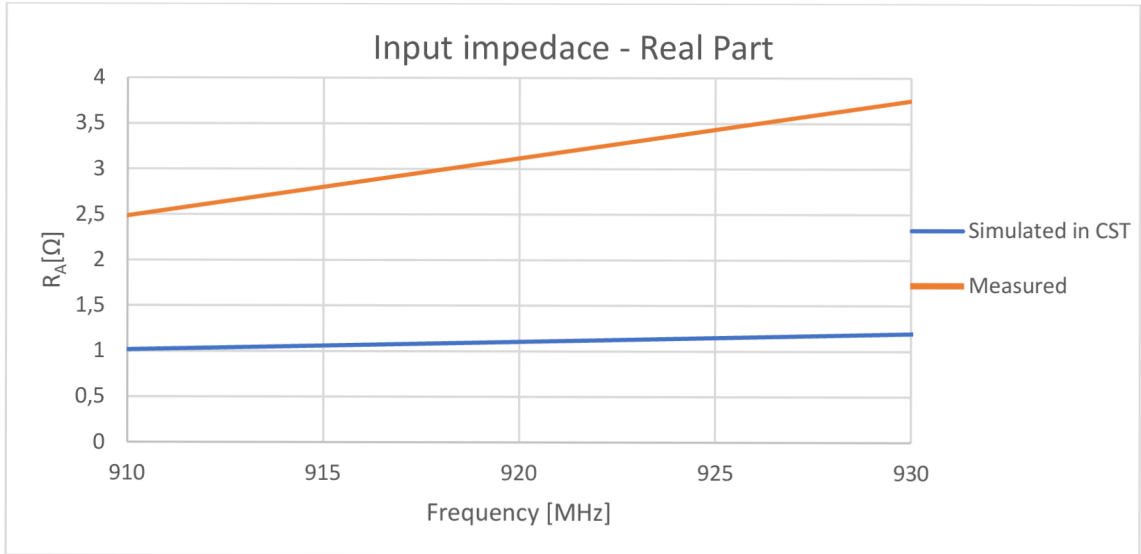


Figure 27: Input impedance of the prototype of Antenna- Real part

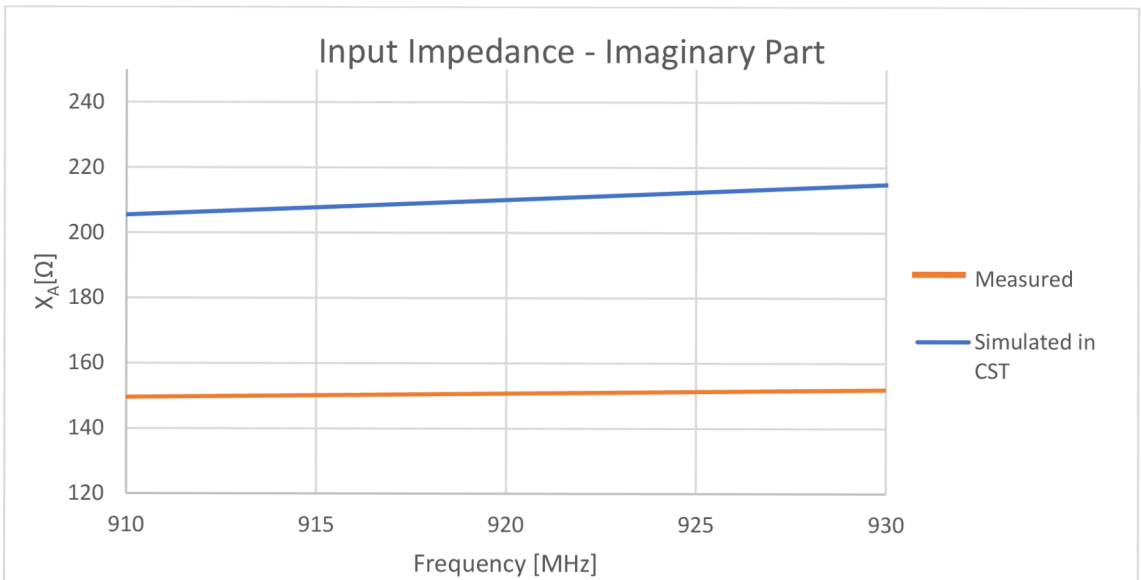


Figure 28: Input impedance of the prototype of Antenna- Imaginary part

The Antenna has been measured without a plastic canister with water. In the figures 27 and 28 we can see, that values of real (R_A) and imaginary (X_A) parts of input impedance are very different at frequency 915 MHz. Target value of the input impedance is $(1+207j) \Omega$ and measured value is $(3.5+146j) \Omega$.

This difference might be given by the inaccurate production of the Antenna. Feeding structure is very sensitive to dimension changes and providing with hand production has high value of manufacturing tolerance. Therefore it was decided, that is necessary to do a new professional prototype PCB.

4.4 PCB Prototype

For this prototype a professional etching method has been used. This achieved prototype could have more accurate results than the first one prototype. Dimensions of the Antenna correspond to values which were achieved in to CST Microwaves Studio which are described above (Table 2.).

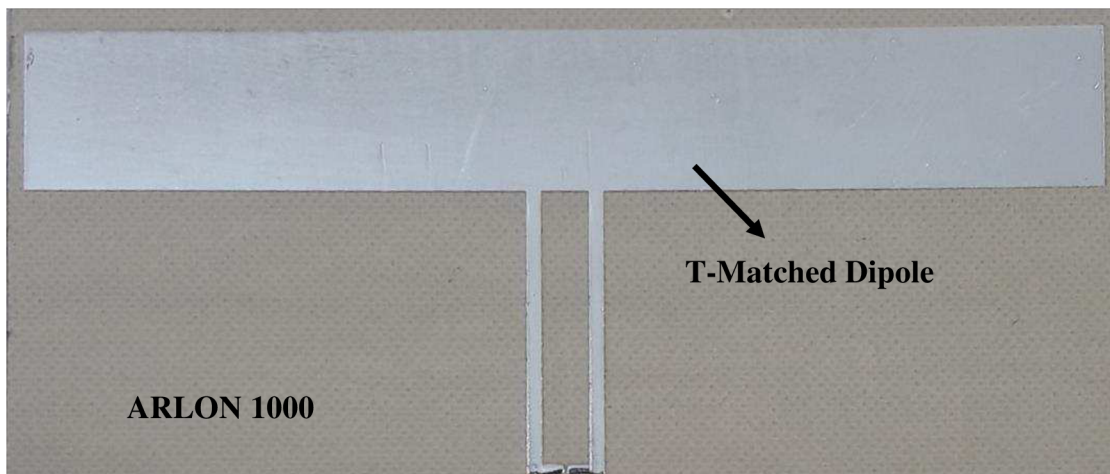


Figure 29: PCB with the Antenna Prototype which was produced by etching method

4.5 Measurement of the second prototype

For measurement the same technique as for the first prototype has been used. For measurement of this prototype a new measure probe has been manufactured. This probe is on substrate FR-4 and gap between feeding structure of the dipole and the probe is corresponding.

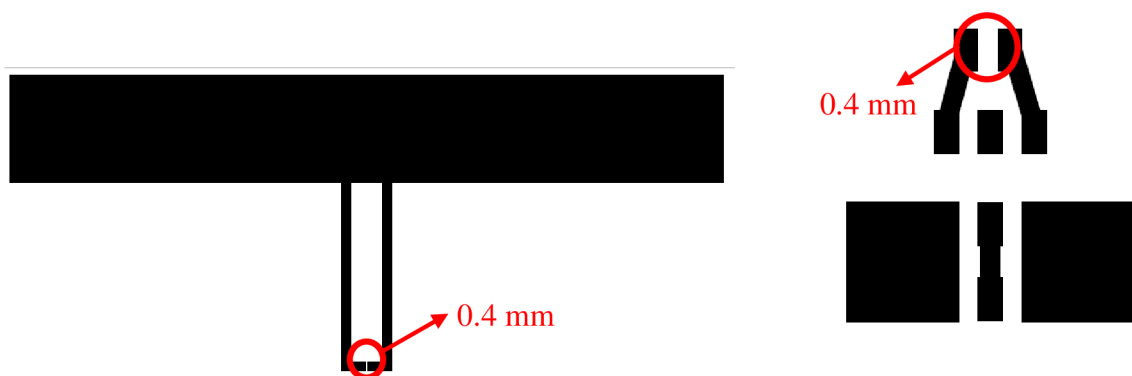


Figure 30: Design of the Antenna and design of the new Measure Probe with the same feeding gap

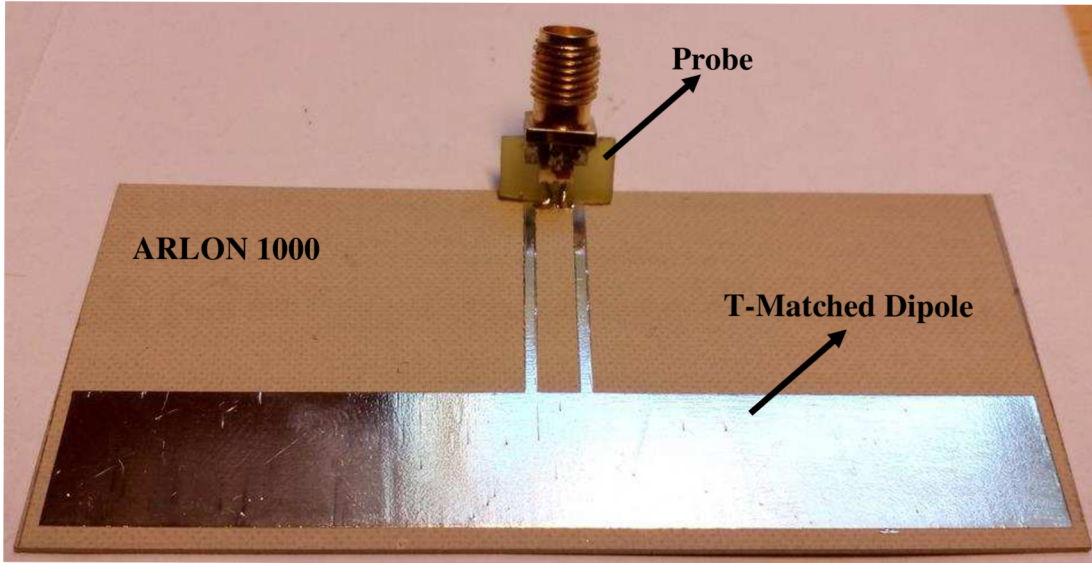


Figure 31: Second prototype of the Antenna with the measurement probe

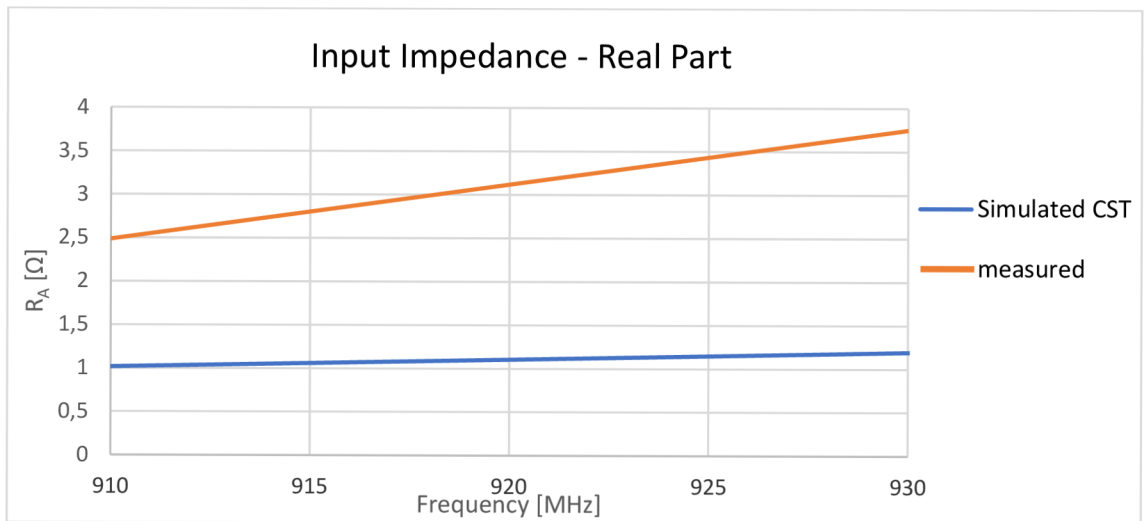


Figure 32: Input impedance of the prototype of Antenna- Real part

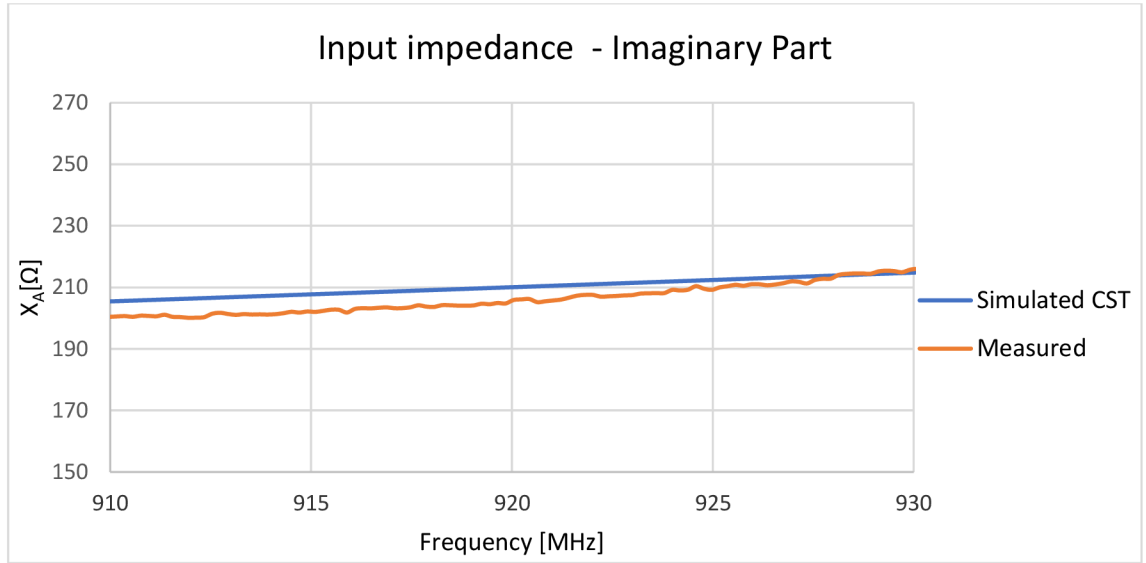


Figure 33: Input impedance of the prototype of Antenna- Imaginary part

Measured values are shown in the Figures 32 and 33. The difference between measured and simulated values is not so critical, as in case of the first prototype. The simulated value for case without plastic canister is $(1+208i) \Omega$ at 915 MHz. The measured value for same frequency is $(2.7+202i) \Omega$. This prototype has been used for final measurement with plastic canister and it was tested, if it is possible to distinguish between two water levels.

5 WATER LEVEL MEASUREMENT

This chapter has described the input impedance measurement of the Antenna prototype which was described above. Measured impedance has been compared with simulated values and shown in the plots.

5.1 Measurement scenario

Measurement scenario is shown in picture 34. For measurement MiniVNA Tiny [10] has been used. The Antenna has been attached to a plastic canister from a PE-HD material. Behind the Antenna the water level was changed and with help of VNA input impedance for each water level has been measured.

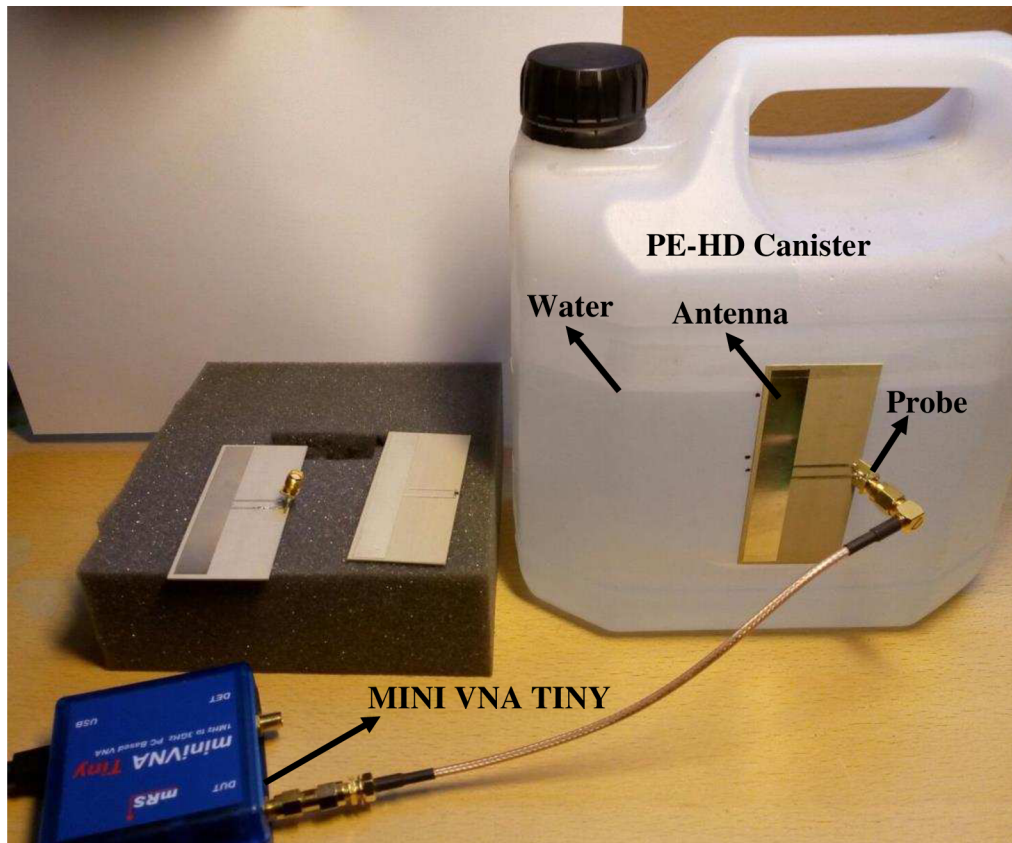


Figure 34: Measurement scenario including MINI VNA TINY, Plastic Canister and Tested Antenna

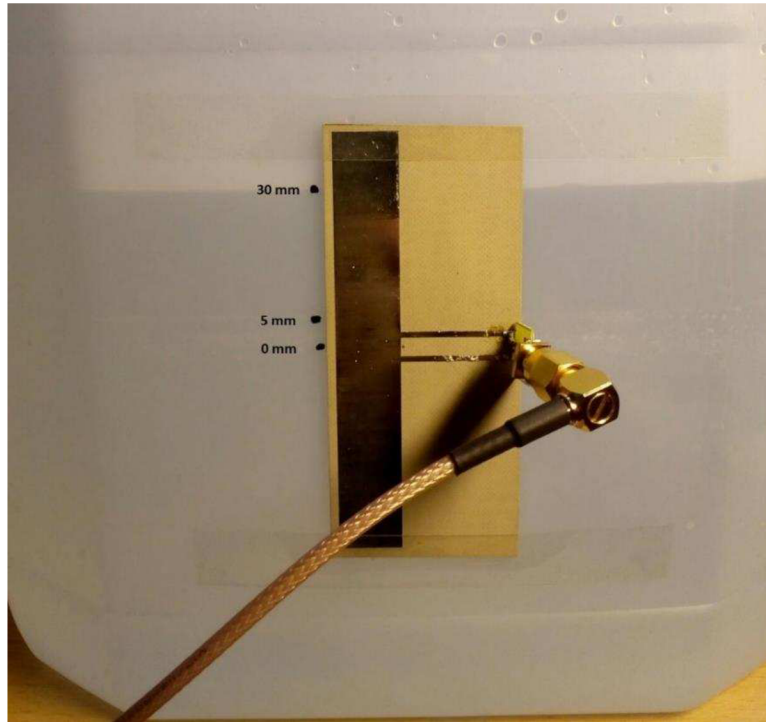


Figure 35: Detail of the Antenna prototype attached on the plastic canister

The Antenna has been attached to the container with the help of a classic plastic tape. Figure 35 shows the detail of the Antenna prototype attached to the plastic container. In the same picture are marks of the required levels (5 mm and 30 mm).

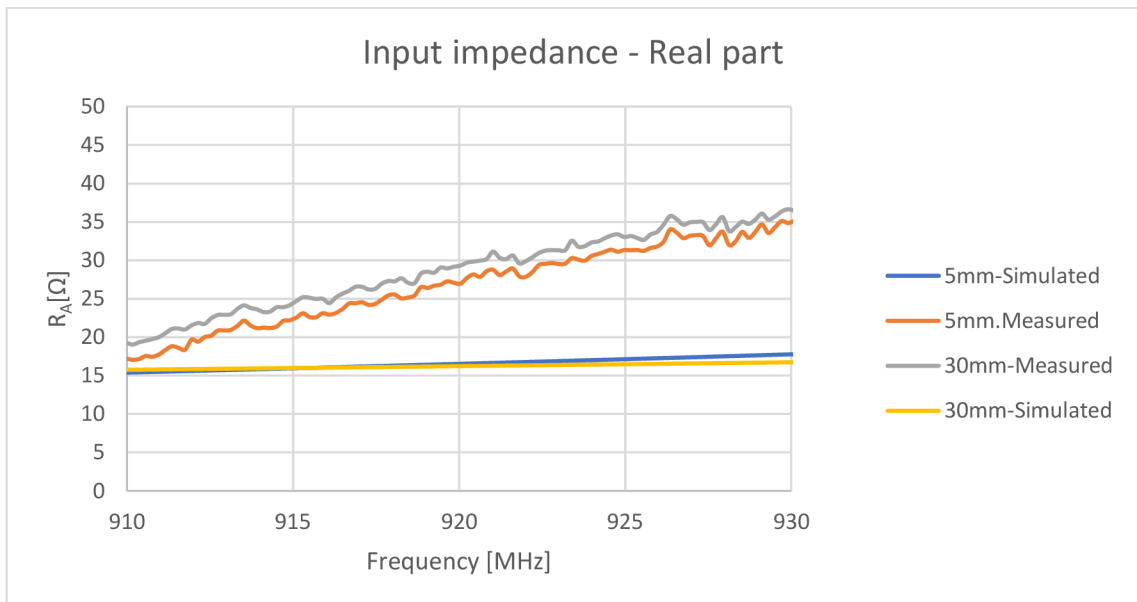


Figure 36: Real part of impedance for two sensing states

For each sensing state a measurement has been done and the results are shown in figures 36 and 37. Figure 36 shows the real value of the input impedance. Expected value of real part for each sensing states were 16 Ω . But the measured results are little bit different. Measured real value for 5mm is 24 Ω and for 30 mm is 25 Ω . On the whole, the real part of impedance is higher than the simulated value.

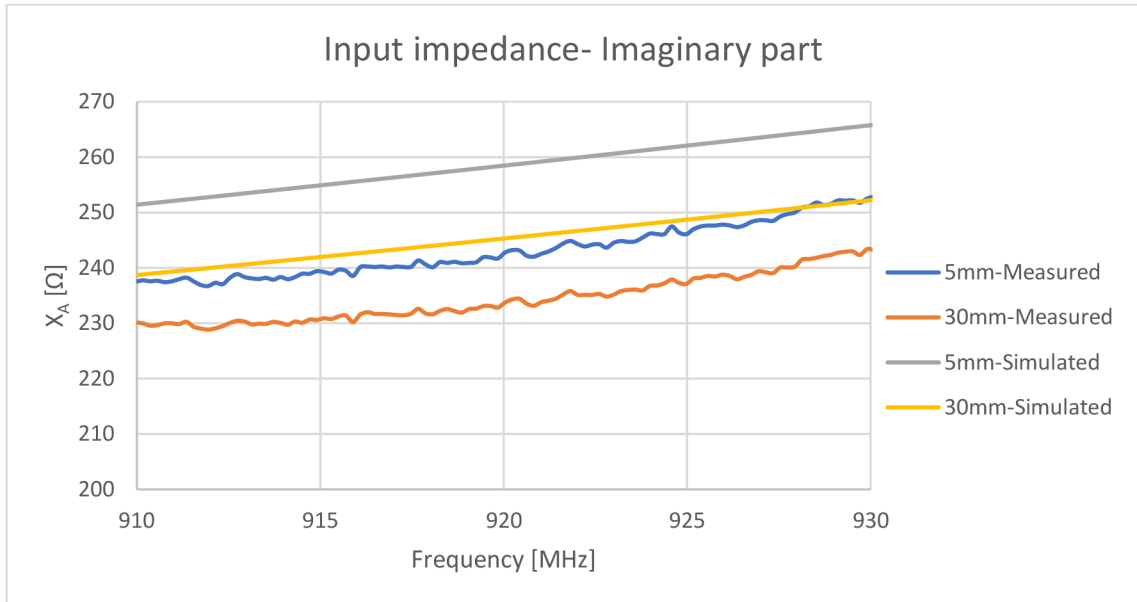


Figure 37: Imaginary part of impedance for two sensing states

For each sensing state the imaginary part is smaller than the expected value. For 5 mm is 240 Ω and for 30 mm 230 Ω . But the difference between both sensing states is 10 Ω . It means that it should still be possible to distinguish between two sensing states.

Table 4: Measured values of the input impedance for both sensing states

| Sensing state | Z_{ant} [Ω] | τ [-] | ϕ_{abs} [$^\circ$] | η [-] |
|---------------|------------------------|------------|---------------------------|------------|
| Δ_1 | 24+240j | 0.883 | 225 | 0.325 |
| Δ_2 | 22+230j | 0.732 | 265 | 0.314 |

The constellation diagram from measurement was obtained which is shown in picture 38. The diagram describes the final situation for two sensing states. The figure shows two real sensing states for levels 5mm (Sabs (Δ_1)) and 30 mm (Sabs (Δ_1)). The phase difference between the two sensing states is 40 $^\circ$.

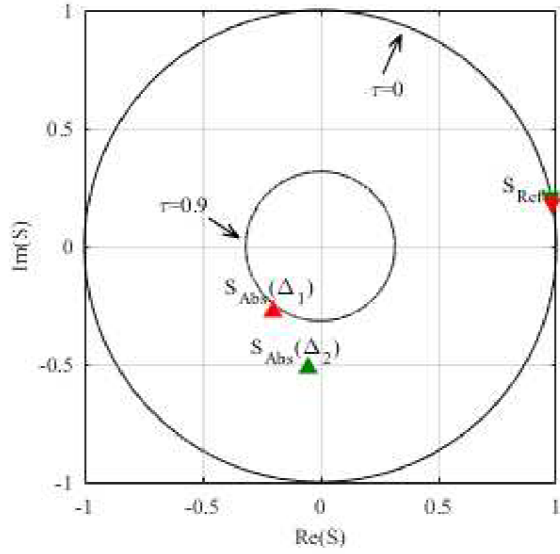


Figure 38: Constellation diagram for final values of Antenna impedances achieved by measurement

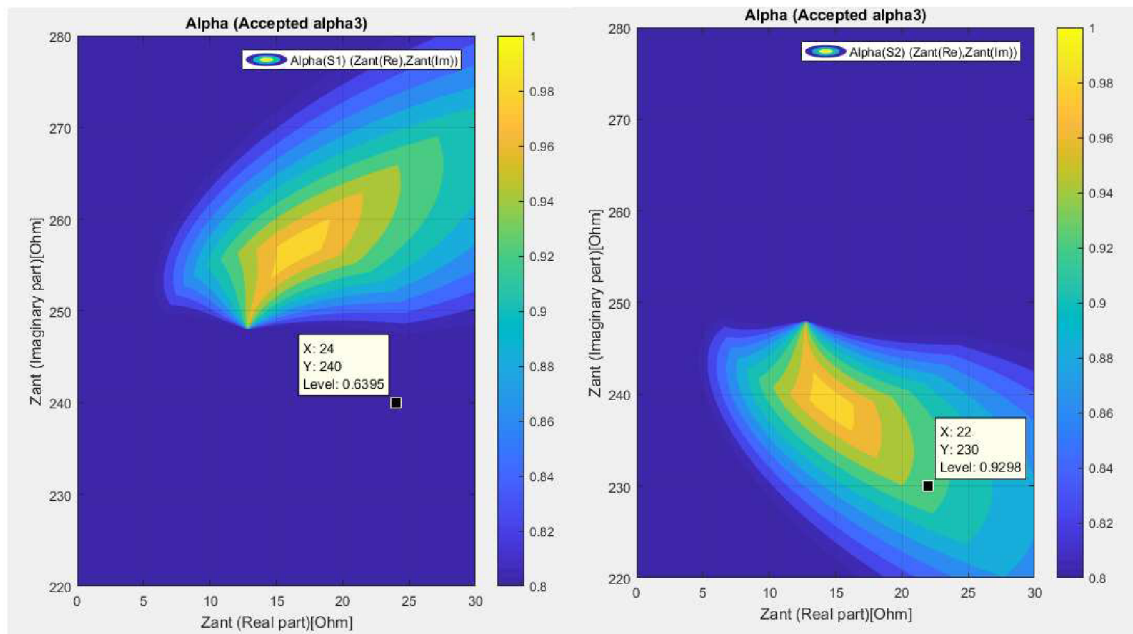


Figure 39: Sensor tag efficiency for both sensing states

Figure 39 shows sensor tag efficiency corresponding with input impedances which was achieved by measurement. Left side of the plot corresponds with first sensing state ($\alpha=64\%$), right side corresponds with second sensing state ($\alpha=93\%$).

5.2 Prototype with RFID chip UCODE 7

The final prototype was attached by UCODE 7 chip provided by NXP. This chip is in package SOT886 with a gap between soldering pads of 0.3 mm. A hot air soldering station was necessary to use for soldering. The final prototype assembled by UCODE 7 chip is shown in picture 40.

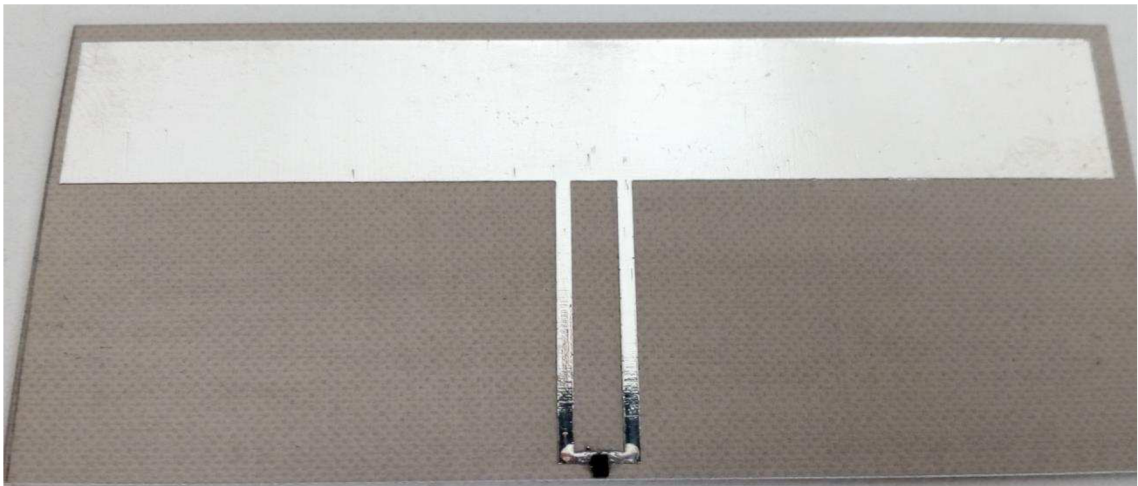


Figure 40: Final prototype with UCODE 7 chip

This prototype was tested with the help of a UHF RFID reader implemented by the Institute of Microwave and Photonic Engineering at TU GRAZ. It was found out that the response of the prototype is very weak. For each sensing state a very weak signal was received, from which it was not possible to define the input impedance of an Antenna.

It could be caused with bad connection between UCODE 7 chip and feeding structure. Another possible cause is inaccurately chosen input impedance of a chip. Value from datasheet can be inaccurate, because was achieved for example with help of simulation. In the Figures 41 ,42 and 43 are shows gains of Antenna for each situation. In other words for situations without a plastic canister with water, with plastic canister and water for sensing state 5 mm and 30 mm.

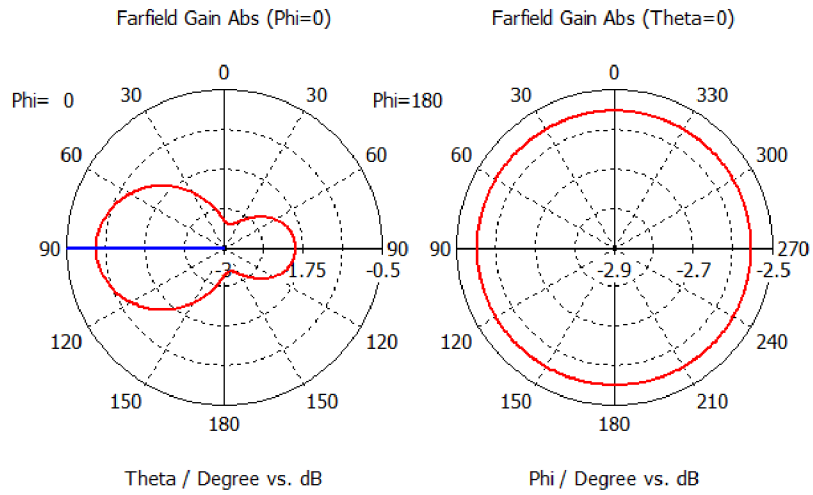


Figure 41: Simulated radiation pattern - Only Antenna , E plane (right), H plane (left)

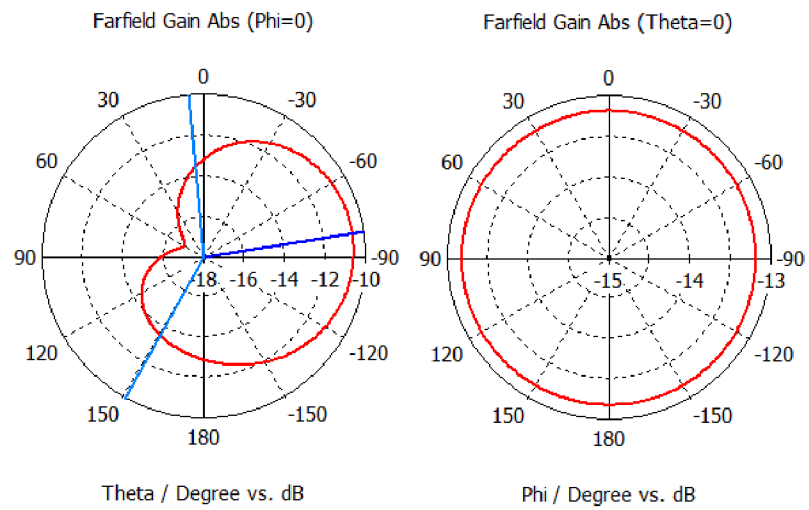


Figure 42: Simulated radiation pattern - Water 5mm , E plane (right), H plane (left)

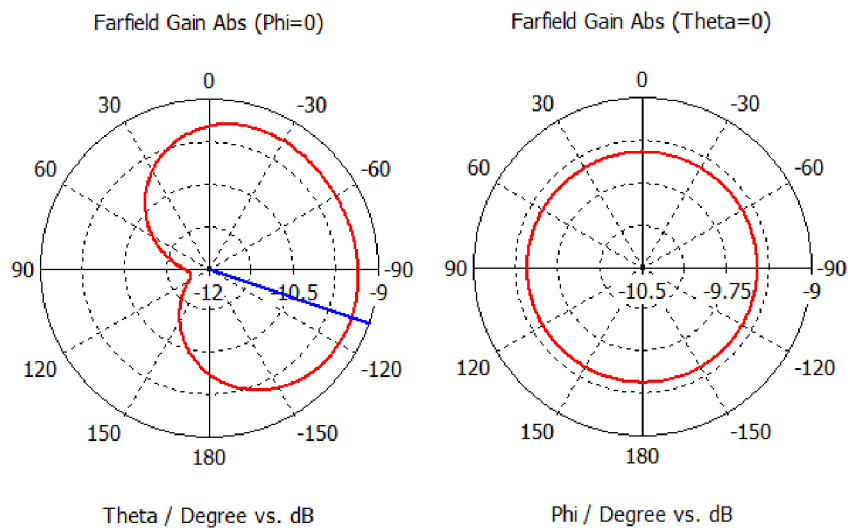


Figure 43: Simulated radiation pattern - Water 30mm , E plane (right), H plane (left)

Figures 40-42 shown gain of the Antenna for different scenarios. Water has very big relative permittivity (around 72). It means, that when is behind an antenna water. So, electromagnetic field is concentrated to the water and total gain is decreases. For higher gain of this system can be uses another type of substrate with smaller relative permittivity like are FR-4 and Rogers

6 CONCLUSION

The project has described the design of the RFID Antenna for measuring liquid levels in plastic containers. In the first part, Matlab script has been presented to compute ideal sensing states for liquid measurement. This script optimizes the sensor tag Antenna impedances with respect to sensor tag efficiency. From that script, theoretical Antenna impedance values have been determined.

Antenna impedances from Matlab were used as input parameters in CST Microwave Studio. In CST, a scenario of complete measurement behaviour has been simulated: we considered Arlon 1000 substrate, PE-HD substrate and water. Furthermore, the influence of water on Antenna input impedance has been investigated. By means of simulation in CST, two input impedance values for two water levels (5 mm and 30 mm) were calculated. There are small differences between optimal results generated by the Matlab script and CST results, but theoretically, the sensor tag efficiency of the RFID transponder is still over 90 %.

Results from simulation have been used for manufacturing of Antenna prototypes. Two prototypes were manufactured, one with help of a copper tape and second with a professional PCB. These prototypes were measured with help of VNA and results were shown in the plots. With help of measurement it was found out that theoretically it is possible to distinguish between two water levels. Phase difference between both impedances is approx. 40 °.

The prototype was assembled with the UCODE 7 chip and tested with help of the special reader. With a reader a very weak signal has been received, from which it was not possible to read information about input impedance. Possible causes have been described above.

Further research should solve issue with connection of UCODE 7 chip, which is designed for a PCB assembly machine. For connection a special conductive glue has been tried, but result was same. However, theoretical design and practical measurement of the transponder Antenna look realistic, therefore should be in next steps investigated, why was received very weak signal.

REFERENCES

- [1] GROSINGER, J., BÖSCH, W. A passive RFID sensor tag Antenna transducer, 8th European Conference on Antennas and Propagation (EuCAP 2014), p. 3638–3639.
- [2] LANDT, J. The history of RFID, IEEE Potentials, 2005, vol. 24, no. 4, p. 8–11.
- [3] GÖRTSCHACHER, L. Design and development of an Antenna transducer for a backscatter RFID sensor tag. Graz: Graz University of Technology, Faculty of Electrical Engineering and Information Technology. Institute of Microwave and Photonic Engineering, 2014. Master Thesis, Supervisor: Dipl.-Ing. Dr. techn. Jasmin Grosinger.
- [4] NXP Semiconductors, Smart Label and Tag ICs, SL3S1204: UCODE® 7 datasheet, Nov. 2017 [Revised March 2017].
- [5] MARROCCO, G, The art of UHF RFID Antenna design: impedance-matching and size-reduction techniques, Antennas and Propagation Magazine, IEEE, 2008, vol. 50, no. 1, p. 66–79.
- [6] LOZANO-NIETO, A. RFID design fundamentals and applications. Boca Raton, FL: CRC Press, 2011. ISBN 1420091263.
- [7] BERRA, F., COSTANZO, A., GROSINGER, J., GÖRTSCHACHER, L. Space mapping design method for an Antenna transducer of a bend sensor RFID Tag, 47th European Microwave Conference.
- [8] Wang, Bo & Zhuang, Yiqi & Li, Xiaoming & Ren, Xiaojiao & Qi, Zengwei & Zhang, Yanlong. (2014). A novel method for impedance measurement of balanced UHF RFID tag Antennas. Journal of Electromagnetic Waves and Applications. 28. 10.1080/09205071.2014.957350.
- [9] JOHANSON TECHNOLOGY, High Frequency Ceramic Solutions, 900 MHz Balun datasheet, Aug. 2004
- [10] MINI RADIO SOLUTIONS, Hardware Manual for miniVNA Tiny, 2014

LIST OF SYMBOLS AND ABBREVIATIONS

| | |
|--------------|---|
| S_{Abs} | Absorption mode |
| S_{Ref} | Reflection mode |
| Z_{Ant} | Antenna impedance |
| Z_{Ref} | Reflection impedance |
| Z_{Abs} | Absorption impedance |
| τ | Transmission coefficient |
| τ_{ref} | Reference transmission coefficient |
| α | The sensor tag efficiency |
| α_1 | Quality of the phase modulation |
| α_2 | Quality of the passive RFID chip power supply |
| α_3 | Quality of the backscattered tag signal |
| β_1 | Weighting factor |
| β_2 | Weighting factor |
| η | Efficiency |
| ϕ_{Abs} | Phase difference |
| Δ_k | Sensing state-k |